NAVAL POSTGRADUATE SCHOOL
Monterey, California

THESIS

A STUDY OF THE EFFECT OF DESIGN PARAMETER VARIATION ON PREDICTED TILT-ROTOR AIRCRAFT PERFORMANCE

by

Mary Cottrell Dunston

December 1988

Thesis Advisor: Richard D. Wood

REPORT DOCUMENTATION PAGE

1a. REPORT SECURITY CLASSIFICATION UNCLASSIFIED	1b. RESTRICTIVE MARKINGS
2a. SECURITY CLASSIFICATION AUTHORITY	3. DISTRIBUTION/AVAILABILITY OF REPORT Approved for public release;
2b. DECLASSIFICATION/DOWNGRADING SCHEDULE	Distribution is unlimited
4. PERFORMING ORGANIZATION REPORT NUMBER(S)	5. MONITORING ORGANIZATION REPORT NUMBER(S)
6a. NAME OF PERFORMING ORGANIZATION Naval Postgraduate School 6b. OFFICE SYMBOL (If applicable) 31	7a. NAME OF MONITORING ORGANIZATION Naval Postgraduate School
6c. ADDRESS (City, State, and ZIP Code) Monterey, CA 93943-5000	7b. ADDRESS (City, State, and ZIP Code) Monterey, CA 93943-5000
8a. NAME OF FUNDING/SPONSORING ORGANIZATION 8b. OFFICE SYMBOL (If applicable)	9. PROCUREMENT INSTRUMENT IDENTIFICATION NUMBER
8c. ADDRESS (City, State, and ZIP Code)	10. SOURCE OF FUNDING NUMBERS PROGRAM ELEMENT NO. / PROJECT NO / TASK NO / WORK UNIT ACCESSION NO.
11. TITLE (Include Security Classification) A Study of the Effect of Design Parameter Variation on Predicted Tilt-Rotor Aircraft Performance	
12. PERSONAL AUTHOR(S) Mary Cottrell Dunston	
13a. TYPE OF REPORT Master's Thesis	13b. TIME COVERED FROM _____ TO _____
14. DATE OF REPORT (Year, Month, Day) December, 1988	15. PAGE COUNT 104
16. SUPPLEMENTARY NOTATION The views expressed in this thesis are those of the author and do not reflect the official policy or position of the Department of Defense or U.S. Government.	

17. COSATI CODES		
FIELD	GROUP	SUB-GROUP

18. SUBJECT TERMS (Continue on reverse if necessary and identify by block number)
Tilt-rotor, Design parameters, Design trade-offs, Disk Loading, Tip speed, Rotor solidity, Download, Wing loading, Wing thickness ratio

19. ABSTRACT (Continue on reverse if necessary and identify by block number)

There is currently little data available for trend analyses of tilt-rotor performance. This study analyzed the sensitivity of predicted tilt-rotor performance to variations in six design parameters: disk loading, tip speed, solidity, download, wing loading, and wing thickness ratio. Two mission profiles were analyzed: A combat search-and-rescue (CSAR) mission and an antisubmarine warfare (ASW) mission. A tilt-rotor preliminary design code (TR-87) was used to perform computer simulations; and data available from independent tests completed by NASA and the military were encoded in the input data decks.

Results were presented as graphs of performance aspects plotted against the parameters varied. Because the study was a trend analysis, no specific conclusions were drawn; but a summary was made of the more significant results. It is hoped that the results of this project can serve as a guide to preliminary selection of design parameters for tilt-rotor configurations that would be suitable for a broad range of military and civil applications.

20. DISTRIBUTION/AVAILABILITY OF ABSTRACT ☒ UNCLASSIFIED/UNLIMITED ☐ SAME AS RPT ☐ DTIC USERS	21. ABSTRACT SECURITY CLASSIFICATION UNCLASSIFIED
22a. NAME OF RESPONSIBLE INDIVIDUAL R. D. Wood	22b. TELEPHONE (Include Area Code) (408) 646-2491/2492 22c. OFFICE SYMBOL 76WR

DD FORM 1473, 84 MAR — 83 APR edition may be used until exhausted. All other editions are obsolete

SECURITY CLASSIFICATION OF THIS PAGE

☆ U.S. Government Printing Office: 1986—606-24.

Approved for public release;
distribution is unlimited.

A Study of the Effect of Design Parameter Variation on
Predicted Tilt-Rotor Aircraft Performance

by

Mary Cottrell Dunston
Lieutenant, United States Navy
B.S., University of Texas, 1979

Submitted in partial fulfillment of the
requirements for the degree of

MASTER OF SCIENCE IN AERONAUTICAL ENGINEERING

from the

NAVAL POSTGRADUATE SCHOOL
December, 1988

Author: Mary Cottrell Dunston
Mary Cottrell Dunston

Approved By: Richard D Wood
Richard D. Wood, Thesis Advisor

E. R. Wood
E. Roberts Wood, Chairman, Department of
Aeronautics and Astronautics

G E Schacher
Gordon E. Schacher, Dean of Science and Engineering

ABSTRACT

There is currently little data available for trend analyses of tilt-rotor performance. This study analyzed the sensitivity of predicted tilt-rotor performance to variations in six design parameters: disk loading, tip speed, solidity, download, wing loading, and wing thickness ratio. Two mission profiles were analyzed: A combat search-and-rescue (CSAR) mission and an antisubmarine warfare (ASW) mission. A tilt-rotor preliminary design code (TR-87) was used to perform computer simulations; and data available from independent tests completed by NASA and the military were encoded in the input data decks.

Results were presented as graphs of performance aspects plotted against the parameters varied. Because the study was a trend analysis, no specific conclusions were drawn; but a summary was made of the more significant results. It is hoped that the results of this project can serve as a guide to preliminary selection of design parameters for tilt-rotor configurations that would be suitable for a broad range of military and civil applications.

TABLE OF CONTENTS

ACKNOWLEDGEMENTS

I wish to thank several individuals for the help I received in completing this project:

Mr. Fort F. Felker	Rotary-Wing Aeromechanics Branch
CDR Hugh Sheehy	NASA-Ames Research Center
Dr. Richard D. Wood	Naval Postgraduate School
Dr. Mike Scully	USA Aviation Research and Technology Activity
Mr. John Davis	NASA-Ames Research Center
CDR Roger Vehorn	Naval Air Systems Command
CDR Steve Fahrenkrog	PMA-275

In addition, I owe my thanks to my husband, Richard, for his continued support, enthusiasm, and understanding.

I. INTRODUCTION

Tilt-rotor technology has arrived. Bell's proof-of-concept research aircraft, the XV-15, made its first successful conversion to forward flight in July of 1977. More recently, on May 23, 1988, the first (of six planned) Bell-Boeing V-22 full-scale development flight aircraft was rolled out.

The V-22 Osprey is unique in many respects. It is also a careful balance of compromises. It will not hover as efficiently as a helicopter or fly horizontally as well as a conventional fixed-wing aircraft. However, it is designed to rise from the ground and hover like a helicopter and then, in 12 seconds, to transition to a relatively fast, fuel-efficient aircraft that can travel at 300 knots for more than 1100 nautical miles. In short, the V-22 represents a significant breakthrough in aeronautical engineering, with incredible potential for future development and usage in both military and civil aviation.

When developing new aircraft, designers vary design parameters to tailor the model to meet performance requirements and constraints. If tilt-rotor technology is to be applied to different applications, designers will need to know which parameters to vary--and by how much--in order to achieve an optimum design for the given mission.

A. ANALYSIS OBJECTIVES

Extensive data bases from existing aircraft are available in both the fixed-wing and rotary-wing communities to allow "trend analysis" to be applied in the

conceptual and preliminary stages of design. It is possible for designers of new aircraft to study historical data in order to predict what gains can be made by varying certain design parameters in terms of increased performance or in meeting mission requirements.

The XV-15 has been subjected to extensive in-flight test and evaluation; and V-22 components have also been exposed to some wind-tunnel and aerodynamic testing. Currently, however, there is relatively little information in the public domain concerning the effect of varying various tilt-rotor design parameters.

The intent of this study is to analyze the sensitivity of predicted tilt-rotor performance to variations in six design parameters:

- disk loading,
- tip speed,
- solidity,
- download,
- wing loading, and
- wing thickness ratio.

The first three parameters are highly interrelated. For the purpose of this paper they will be grouped together as "rotor characteristics" for initial discussion. The last two parameters will be considered as purely "aircraft characteristics", and will be discussed separately. Downloaad is a function of both the rotor characteristics and wing geometry, but will be discussed in the section on rotor characteristics.

As test data from the V-22 becomes available it will be added to the existing data base and compared to the results of computer analyses of predicted

performance. As that occurs the computer codes used for tilt-rotor analysis can be verified and/or refined. In the interim, it is hoped that analysis of the interdependence of these parameters will help to establish general performance trends and, ultimately, facilitate design optimization of future-generation tilt-rotor aircraft.

B. APPROACH

Tilt-rotor aircraft represent the melding of two technologies: one developed for conventional aircraft and one developed for rotary-wing aircraft. In addition to design trade-offs inherent in the design of any aircraft, a tilt-rotor aircraft's duality of nature results in dramatic compromises between its high-speed forward flight (conventional) and its low-speed/hover (rotary-wing) mode of flight. Therefore, two representative Navy missions were selected for this study. A combat search-and-rescue (CSAR) mission was chosen to demonstrate high-speed performance; and an antisubmarine warfare (ASW) mission was chosen for the low-speed/hover regime.

In order to perform a parametric analysis of tilt-rotor technology, it was necessary to use a computer code that was capable of predicting both conventional and rotary-wing modes of behavior. The code used for this study was designed specifically for preliminary design of tilt-rotor aircraft. However, rather than using the code for design of an aircraft, it was manipulated for parametric analysis using the V-22 Osprey as a baseline aircraft. This was accomplished by encoding two sets of input data decks (one for each mission) with the V-22's engines, rotors, and geometric configuration as design constraints and allowing other parameters to fall

out. The two data decks were then re-coded to vary the six parameters of interest independently.

A note on philosophy and methodology should be included here. Every effort was made to include in the input data decks as much information about the V-22 as was known at the time. Otherwise, data from XV-15 tests was used and scaled for differences in the two aircraft configurations. The lack of absolute precision should not adversely affect the results of this study. While it is hoped that this analysis will predict the actual performance of the V-22 fairly closely, the goal is not necessarily to predict absolute levels of performance. Rather, the analysis will focus on predicted trends of tilt-rotor performance and effects of design changes from baseline design.

II. TILT-ROTOR PRELIMINARY DESIGN CODE (TR-87)

As mentioned previously, the computer code used for this analysis is a preliminary design code specifically developed for tilt-rotor aircraft. This code, currently known as TR-87, was developed jointly by the U.S. Army Aviation Research and Technology Activity (ARTA) and the NASA Advanced Plans and Programs Office at Ames Research Center. The code has been continually updated with data correlation since it was first introduced. The "87" appended to the name refers to the year 1987, when the last major revision of the code was implemented.

References 1 and 2 describe the computer code in some detail. As a brief description, TR-87 is a comprehensive, state-of-the-art synthesis design code that takes a given set of mission requirements, constraints, engine characteristics, and design configuration decisions and determines the size, component weights and flight performance of the resulting aircraft design. The code has been extensively correlated with available experimental data as well as predictions of rotor performance obtained from a separate rotorcraft analysis code known as CAMRAD (Comprehensive Analytical Model of Rotorcraft Aerodynamics and Dynamics).

> The synthesis design code predicts the hover, conversion, and airplane-mode performance for steady-state, level-flight conditions. The mission performance is computed with a series of hover and forward-flight segments flown for an input time or distance, with mission fuel computed as the sum of fuel burned for each segment. Off-design mission performance can also be determined. [Ref. 2, p. 15-7]

Human intervention is required to evaluate practical operating concerns. For example, shipboard compatibility must be evaluated before the input data deck is

encoded in order to put constraints on size or given geometric parameters. Noise and environmental impact can be judged by evaluating such output data as tip speed and rotor-induced velocity. Also, the output of the code is highly dependent on the accuracy of the data and empirical factors that are input. In spite of these limitations (which are inherent in any computer code), TR-87 could be a highly valuable tool in the design of future aircraft.

A. MISSION GROSS WEIGHT LOOP

Weight estimates for aircraft components are calculated by correlating experimental data and statistical trends with dimensions/geometry of the input aircraft configuration. The weight-trend equations are based on existing aircraft designs, including the Bell XV-15. In addition, advanced technology factors (ATF) are applied to reflect special design features such as the use of composite materials, fly-by-wire (FBW) control systems, advanced drive system technology, oversized canopy for improved landing visibility, blade-folding mechanisms, and landing gear capable of kneeling for improved shipboard compatibility. Technology factors for different components are included in Tables 3 and 6; these are the ratio of the component weight using advanced technology to component weight using conventional technology. In each iteration, the estimated component weights are summed to yield an estimated empty weight. Payload, crew weight, fixed useful loads, and estimates of fuel weight (based on fuel flow characteristics of the engines used) are added in to yield estimated mission gross weight. This value of mission gross weight is used as a starting point for determining rotor characteristics.

Revised estimates for weights, power required, and fuel flow are made based upon the fallout rotor characteristics. (Some of these characteristics can be fixed values if the input deck is coded to hold a certain parameter at the input value: This is exactly how variations were made in the parameters of interest for this study.) The iterative loop process is continued until the gross weight converges and mission requirements/constraints are met.

B. ROTOR PERFORMANCE

Rotor aerodynamic performance is estimated using various simplified physical/math models. Throughout his book [Ref. 3] Johnson provides a thorough discussion of the theories behind these models and how they are typically incorporated in a design code. In order to improve the accuracy of the models in predicting actual behavior, they are calibrated by both test data and detailed performance analyses using CAMRAD. This calibration is generally in the form of empirical constants contained within the equations of the analytical models. The data base for blade section aerodynamic characteristics include tests performed on the XV-15 rotor blades and a 0.658-scale model of the V-22 rotor system at the Outside Aerodynamic Research Facility (OARF) at Ames Research Center [Ref. 4]. This test data gives detailed flow and loading of the blades and, hence, relates rotor performance to the detailed design parameters. Rotor-induced power is predicted from combined Momentum-Blade Element theory with non-uniform inflow and tip loss factors applied. Rotor profile power is predicted as a function of blade loading (CTSIGMA) with corrections for advance ratio effects. High-speed corrections for

compressibility effects on both the wings and rotors are applied based on input ambient conditions.

C. WING AND STRUCTURE

Wing and pylon stiffness of a tilt-rotor aircraft are dictated by aeroelastic stability requirements rather than by bending moment criteria. [Ref. 2, p. 15-6] In TR-87, aeroelastic stability margins are estimated based on trends from XV-15 flight and wind-tunnel test data; and the resulting stiffness requirements are then computed. In addition, the code checks to ensure that a 2-g jump takeoff requirement is met. Wing-induced drag is computed as a function of wing coefficient of lift and aspect ratio; and hover download is computed as a function of rotor and wing geometry. Other structural properties, such as mode shapes, are the result of detailed design. Since modal analysis of the V-22 had not been completed at the time of this study, the dynamic characteristics of the XV-15 were used as a baseline, with appropriate changes to reflect stiffness of advanced composites, wing tip mass and inertia, rotor pre-cone angle, and rotor control system stiffness.

D. PROPULSION SYSTEM

Propulsion performance is predicted from curve-fitted models and data for uninstalled thrust provided by the engine's manufacturer (Allison). These models include tabulated engine power, fuel flow, airflow, and tailpipe thrust for given power settings, engine revolutions-per-minute (rpm), flight speed, altitude, and ambient temperature. The input engine performance is corrected for losses due to power transmission, accessory power extraction, and infrared suppression (IRS). For

both the conventional and helicopter modes of flight predictions of performance are largely a matter of determining the power required to balance aerodynamic forces and power available over a range of flight conditions.

III. MISSION PROFILES

In early (February-May) 1982, the Department of Defense conducted a Joint Vertical Lift (JVX) Joint Technology Assessment (JTA, in conjunction with a conference to develop Joint Services Operation Requirements (JSOR). The purpose of the JVX JTA was to assess the technical feasibility of developing a common-design V/STOL aircraft capable of performing ten defined JSOR missions. Several configurations were considered: single main rotor helicopters (with and without auxiliary wings), auxiliary propulsion compounds (winged and Advancing Blade-Concept versions) tilt-rotor aircraft, and lift/cruise fan aircraft. The findings of the study were presented in May, 1983. The summary report contained the following conclusion: "Thus there is at least one design configuration (tilt rotor) which can satisfy all of the JSOR mission requirements with a high degree of inter-service commonality" [Ref.1, paragraph 9.4.3]. As a result of the JVX JTA study, the V-22 was developed for use by all four U.S. armed services. The fact that the aircraft was designed as an "all-purpose" aircraft implies that it was not optimized for any particular mission. In this study two particular mission profiles were selected for analysis.

A. NAVY COMBAT SEARCH AND RESCUE (CSAR) MISSION

The Navy CSAR mission was identified as one of the ten JSOR missions in the JVX JTA summary report. Pictorial and tabulated representations of the desired mission profile were outlined as Mission 1D [Ref. 1] and are presented in Figure 1

and Table 1. Briefly, the mission calls for the V-22 to take off from a ship with a crew of four, fly 400 nautical miles (nm) inland to rescue four downed aircrewmen, and fly with the rescued crewmen back to the ship, all under extreme (sea level, 103 degrees F) conditions. No required climb performance was specified; but a climb rate of 500 feet per minute was chosen arbitrarily for this analysis. One-Engine-Inoperative Performance was calculated for 3000 ft. altitude, 91.5 degrees F. In order to maximize survivability of the aircraft, crew, and survival victims the mission tests the high-speed/dash capabilities of the aircraft. V-22 data and information from Table 1 was used to encode the DASH baseline data deck. Significant characteristics and weights for the fallout baseline aircraft are presented in Tables 2 and 3.

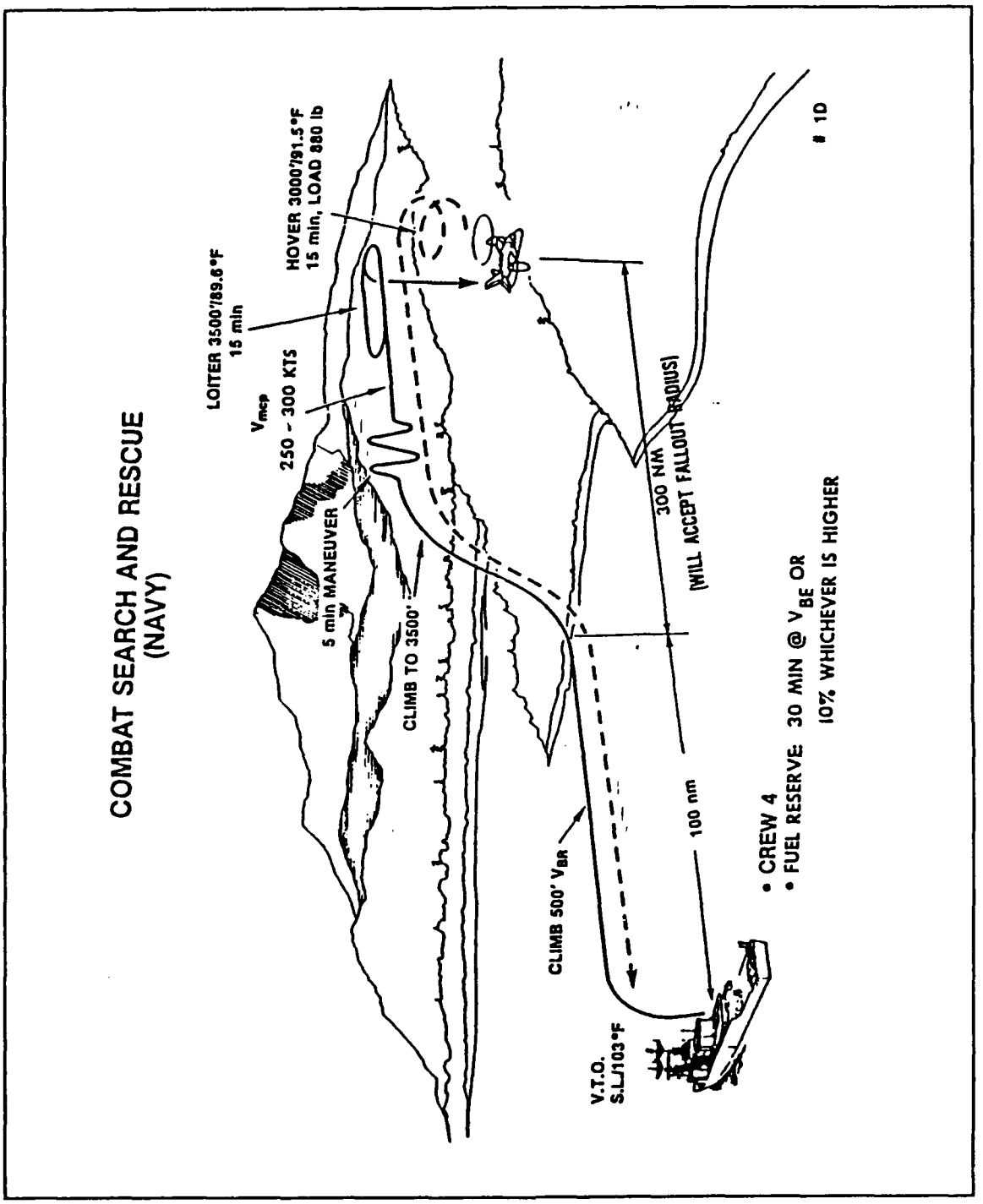

Figure 1

Navy CSAR Mission

TABLE 1

JVX CSAR MISSION PROFILE

SEG NO	ACTIVITY	h (ft)	T (F)	AIRSPEED (knots)	TIME (min)	DISTANCE (nm)	PAYLOAD (lbs)	POWER	VROC (fpm)	IR SUPPRESSOR
1	Idle	SL	103	0	10	0		Idle		OFF
2	Hover/VTO	SL	103	0	1	0		95% IRP	500	OFF
3	Climb	SL	103	V_{CLB}		COC		IRP		OFF
4	Cruise	500	101.1	V_{BR}		100				OFF
5	Climb	500	101.1	V_{CLB}		COC		IRP		ON
6	Cruise	3000	91.5	V_{MCP}		300		MCP		ON
7	Maneuver	3000	91.5		5	0		IRP		ON
8	Loiter	3000	91.5	V_{BE}	15	0				ON
9	Hover	3000	91.5	0	15	0	880	95% IRP		ON
10	Maneuver	3000	91.5		5	0	880	IRP		ON
11	Cruise	3000	91.5	V_{MCP}		300	880			OFF
12	Descend	3000	91.5	300		DOC	880			OFF
13	Cruise	500	101.1	V_{BR}		100	880			OFF
14	Descend	500	101.1	V_{BR}		DOC	880			OFF
15	Reserve	SL	103	V_{BE}	30		880			OFF

TABLE 2

CSAR BASELINE AIRCRAFT CHARACTERISTICS

Disk loading (psf)	19.95
Rotor Diameter (ft)	38.0
Blade chord (in)	25.07
Number of blades	3
CT/SIGMA	0.1389
Solidity (SIGMA)	0.1050
Blade Aspect Ratio	9.1
Overall Width (ft)	83.8
Fuselage Length (ft)	57.3
Fuselage width at rotors (ft)	7.71
Engine No./size	2 x 6345
Engine rated HP (SL/STP/IRP)	12690
Transmission rated HP (15000 rpm)	9150
Power loading (lb/hp)	3.57
Download/Thrust (percent)	11.10
Hover induced velocity (fps)	72.31

	Hover	Cruise
Tip speed (ft/sec)	790	662
Rotor RPM	397	333
Transmission rated HP	9150	7667
Pylon D/Q (sqft)	154.50	4.50

	Wing	Flaperon
Area (sqft)	381.9	35.7
Span (ft)	45.8	17.1
Chord (ft)	8.33	2.08
Thickness(ft)	1.92	
Aspect ratio	5.50	
Thickness/chord	0.23	
Wing Loading (psf	118.5	

TABLE 3

CSAR BASELINE WEIGHTS

WEIGHT GROUP	LB	TECH FACTORS
Wing	3437.0	ATW 0.83
Rotor Blades	1707.5	ATR 0.98
Hub & Hinge	1609.4	ATH 0.89
V/H Tail	854.0	ATT 1.20
Body	5609.6	ATB 0.90
Landing Gear: Wheel	1207.9	ATL 1.28
Cowl & Nacelle	1522.4	ATC 1.58
Engine (Dry)	1953.2	ATE 1.00
GB + RS + RB (RB: 48.3)	3263.4	TGB 0.87
Drive Shafts	306.8	TDS 1.02
Propulsion Subsystems	158.9	TPS 0.78
Exhaust System	479.5	ATX 1.00
Fuel Tanks	607.8	ATK 0.40
Fuel System	379.2	ATG 1.00
Cockpit Controls	55.0	TCC 0.50
Auto Flight Control	118.0	AFC 0.40
Rotor Control	1181.8	ATF 0.57
Conversion System	634.4	ACV 0.64
Fixed Wing Control	547.2	AFW 0.94
Airframe Equipment	3390.9	
Mission Equipment	1000.0	
Contingency	706.6	
Empty Weight	30723.8	
Fuel Burned (3.78 hr)	11632.3	
Fuel Reserve (0.5 hr)	993.5	
Trapped Fluids	64.0	
Crew	880.0	
Fixed Useful	81.0	
Payload (4 survivors)	880.0	
Mission Gross Weight	45254.7	
Weight for Maximum Effort TO	47500.0	

B. NAVY ANTISUBMARINE WARFARE (ASW) MISSION

The ASW mission was not as clearly defined as the CSAR mission and, in addition, had to be modified for this analysis. Figure 2 is a copy of the desired mission profile as received from the SV-22 (ASW version) project manager at Naval Air Systems Command. The mission requires the aircraft to take off at a gross weight of 53,000 pounds from one ship in a task group and fly 250 nm to land on a forward-deployed picket ship. After a 20-minute hot-refuel period, the crew flies 100 nm to prosecute a submarine, spends two and one-half hours on station, returns to the picket ship and, ultimately, the original ship. Time on station is spent loitering and hovering to dip a sonar in the water, testing the low-speed/hover performance of the aircraft.

The ASW mission profile was modified before it was input to the HOVER baseline data deck. For instance, the payload was decreased significantly for three reasons:

- Under the extremely hot conditions used for analysis, the computer code predicted that the aircraft was underpowered for the heavier payload;
- The specified mission gross weight exceeded the current configuration's structural design gross weight and maximum weight for takeoff; and,
- In order to compare the two missions meaningfully, it was desireable to have the fallout baseline configurations be as similar to each other as possible.

Because of the third reason, the input payload and mission equipment weight for the ASW mission were varied until the fallout mission gross weight and disk loading of the baseline aircraft were comparable to those of the CSAR baseline aircraft. A second modification was that the flight segments between the original ship and the

picket ship were ignored in order to concentrate on the low-speed and hover aspects of the mission. Finally, the original mission profile did not specify altitude or temperature: For the sake of comparison, the same extreme ambient conditions and vertical rate of climb were selected as were used for the CSAR mission profile. Table 4 shows the ASW mission profile as it was input to the baseline data deck. Significant characteristics and weights for the baseline ASW aircraft are presented in Tables 5 and 6.

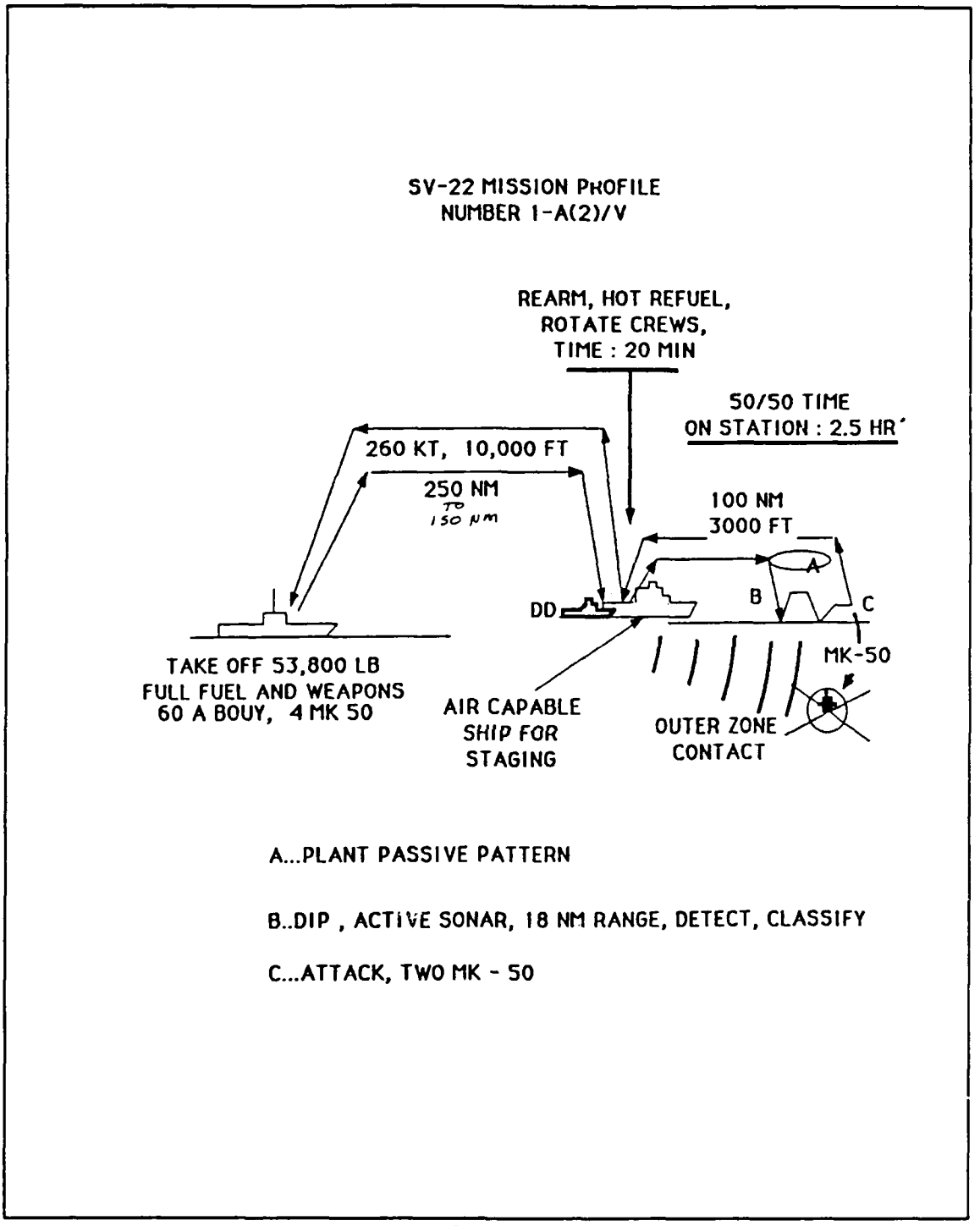

Figure 2

Navy ASW Mission

TABLE 4

SV-22 (ASW) MISSION PROFILE

SEG NO	ACTIVITY	h (ft)	T (F)	AIRSPEED (knots)	TIME/DISTANCE (min)	(nm)	PAYLOAD (lbs)	POWER	VROC (fpm)	IR SUPPRESSOR
1	Idle	SL	103	0	20	0	1500	Idle		OFF
2	Hover/VTO	SL	103	0	1	0	1500	95% IRP	500	OFF
3	Climb	SL	103	V_{CLB}		COC	1500	IRP		OFF
4	Cruise	3000	91.5	V_{BR}		100	1500			ON
5	Cruise	3000	91.5	V_{BE}	70		1500			ON
6	Descend	3000	91.5	250		DOC	1500			ON
7	Hover	250	102	0	70		1210	95% IRP		ON
8	Hover/ Maneuver	250	102	0	10		1210	IRP		ON
9	Climb	250	102				1210	95% IRP	500	ON
10	Cruise	3000	91.5	V_{BE}		100	680			ON
11	Descend	3000	91.5	V_{BE}		DOC	680			OFF
12	Reserve	SL	103	V_{BE}	30		680			OFF

TABLE 5

ASW BASELINE AIRCRAFT CHARACTERISTICS

Disk loading (psf)	19.96
Rotor Diameter (ft)	38.0
Blade chord (in)	25.07
Number of blades	3
CT/SIGMA	0.1390
Solidity (SIGMA)	0.1050
Blade Aspect Ratio	9.1
Overall Width (ft)	83.8
Fuselage Length (ft)	57.3
Fuselage width at rotors (ft)	7.71
Engine No./size	2 x 6345
Engine rated HP (SL/STP/IRP)	12690
Transmission rated HP (15000 rpm)	9150
Power loading (lb/hp)	3.57
Download/Thrust (percent)	11.10
Hover induced velocity (fps)	72.31

	Hover	Cruise
Tip speed (ft/sec)	790	662
Rotor RPM	397	333
Transmission rated HP	9150	7667
Pylon D/Q (sqft)	154.50	4.50

	Wing	Flaperon
Area (sqft)	381.9	35.7
Span (ft)	45.8	17.1
Chord (ft)	8.33	2.08
Thickness(ft)	1.92	
Aspect ratio	5.50	
Thickness/chord	0.23	
Wing Loading (psf	118.5	

TABLE 6

ASW BASELINE WEIGHTS

WEIGHT GROUP	LB	TECH FACTORS
Wing	3437.0	ATW 0.83
Rotor Blades	1707.5	ATR 0.98
Hub & Hinge	1609.4	ATH 0.89
V/H Tail	854.0	ATT 1.20
Body	5609.6	ATB 0.90
Landing Gear: Wheel	1207.9	ATL 1.28
Cowl & Nacelle	1522.4	ATC 1.58
Engine (Dry)	1953.2	ATE 1.00
GB + RS + RB (RB: 48.3)	3263.4	TGB 0.87
Drive Shafts	306.8	TDS 1.02
Propulsion Subsystems	158.9	TPS 0.78
Exhaust System	479.5	ATX 1.00
Fuel Tanks	556.2	ATK 0.40
Fuel System	379.2	ATG 1.00
Cockpit Controls	55.0	TCC 0.50
Auto Flight Control	118.0	AFC 0.40
Rotor Control	1181.8	ATF 0.57
Conversion System	638.4	ACV 0.64
Fixed Wing Control	547.2	AFW 0.94
Airframe Equipment	3390.9	
Mission Equipment	1800.0	
Contingency	706.6	
Empty Weight	31489.8	
Fuel Burned (3.78 hr)	10267.2	
Fuel Reserve (0.5 hr)	997.0	
Trapped Fluids	64.0	
Crew	880.0	
Fixed Useful	81.0	
Payload:		
2 Torpedoes @ 530 lbs each		
15 Sonobouys @ 29 lbs each	1500.0	
Mission Gross Weight	45269.0	
Weight for Maximum Effort TO	47500.0	

C. BASELINE AIRCRAFT PERFORMANCE

Figures 3 through 6 illustrate components of horsepower required against forward airspeed. In this aspect, the two aircraft were identical; therefore, only one set of curves is shown to represent both missions.

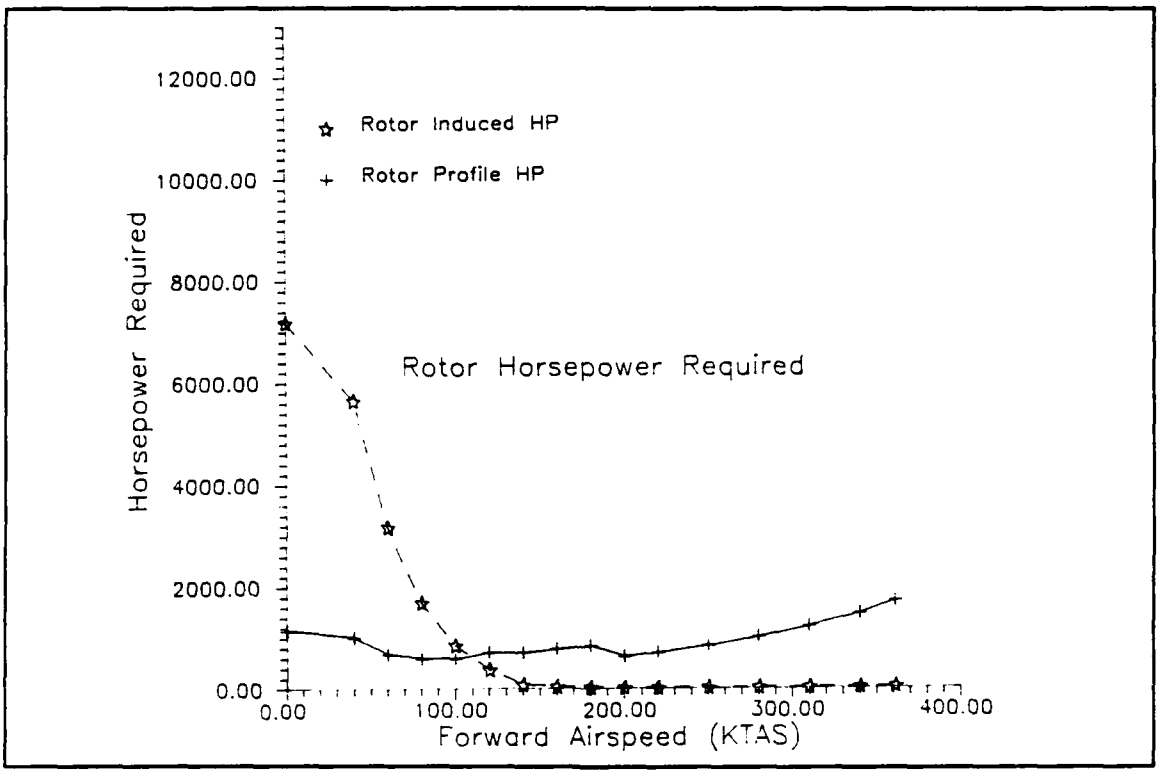

Figure 3

Rotor Power Required

Figure 3 represents plots of induced and profile power for the rotor systems. The graphs look very similar to "typical" curves presented in any helicopter performance book. Induced power is highest for hover and then drops off rapidly with increasing forward airspeed; Profile power increases slightly with increasing advance ratio. However, unlike curves for helicopters, the tilt rotor's induced power

drops off to zero. One possible explanation for the zero values at higher forward airspeeds is the fact that the rotors unload as the aircraft's wings begin providing lift; after transition to forward flight the rotors provide propulsion but no lift. Note also the slight dip in profile power that occurs between 180 and 200 knots, corresponding to transition to forward flight (i.e., rotation of the rotors to the vertical plane) and the subsequent reduction in rotor rpm.

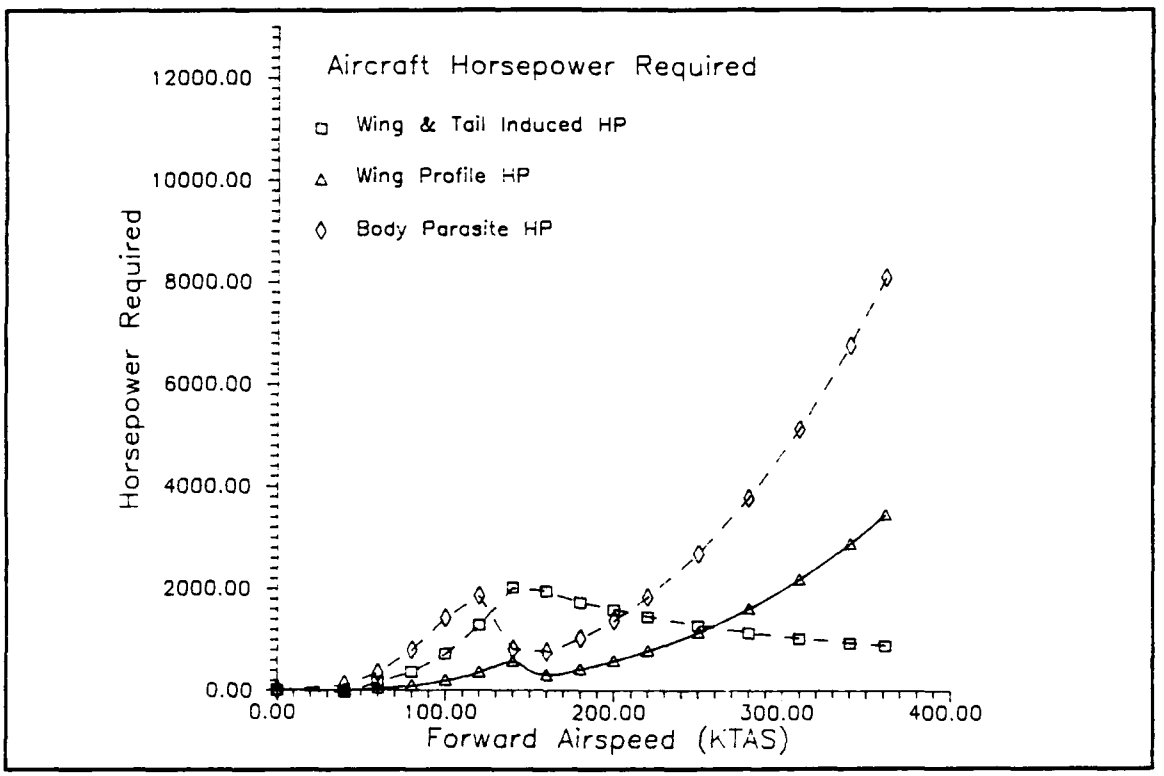

Figure 4

Aircraft Power Required

Various components of aircraft horsepower required are presented in Figure 4. Above 180 knots the curves of induced, profile, and parasite power follow general trends for conventional aircraft performance. Below transition airspeed, however, it

appears that the position of the rotors has some impact on the aircraft power required. The explanation for the behavior of wing and tail induced power is the reverse side of the behavior of rotor induced power presented in Figure 3. As airspeed increases from zero, wing-induced losses increase to the point where the wings are providing all of the lift; after that point, wing-induced losses drop off with continued increases in airspeed in a manner typical of conventional aircraft. The profile power has a relative maximum that occurs in the transition airspeed range. The probable reason for the drop in parasite drag between 100 and 160 knots is a reduction in rotor pylon flat plate drag area during transition.

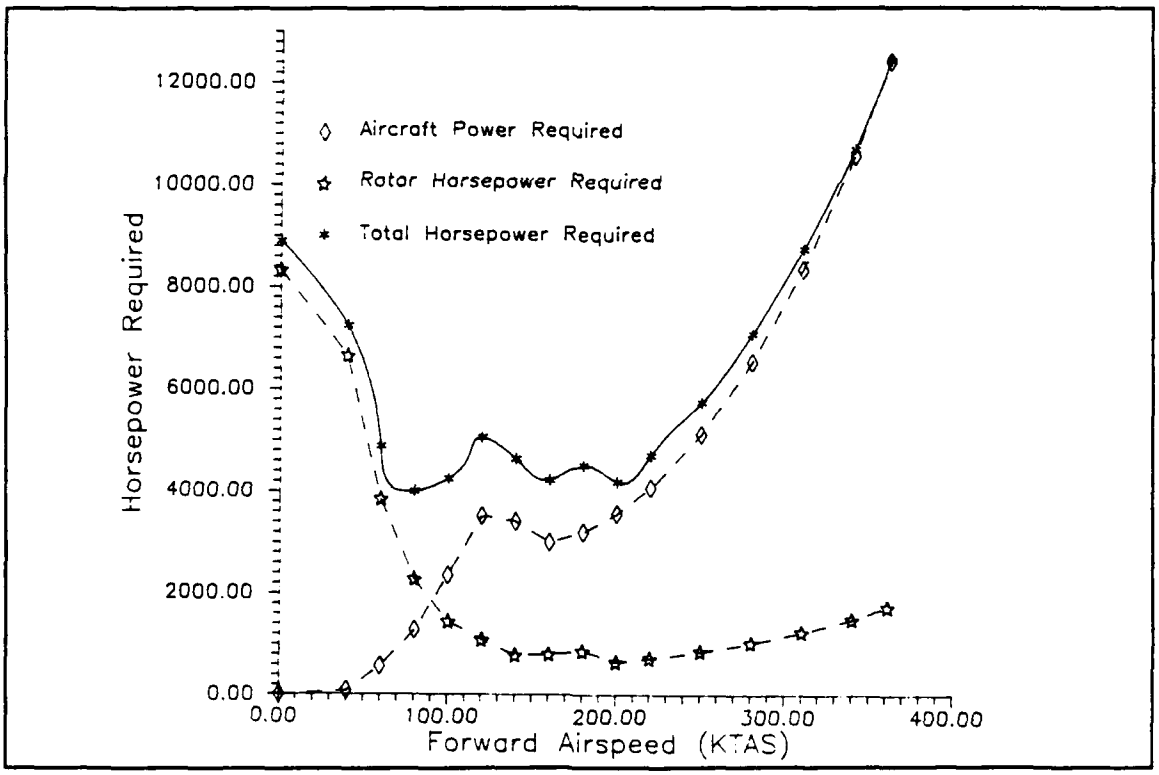

Figure 5

Total Power Required

In Figure 5 the rotor horsepower required curve is the sum of the required power curves in Figure 3; similarly, the aircraft power required is the sum of the individual curves in Figure 4. For all practical purposes, the total horsepower required is the sum of the rotor and aircraft power required.

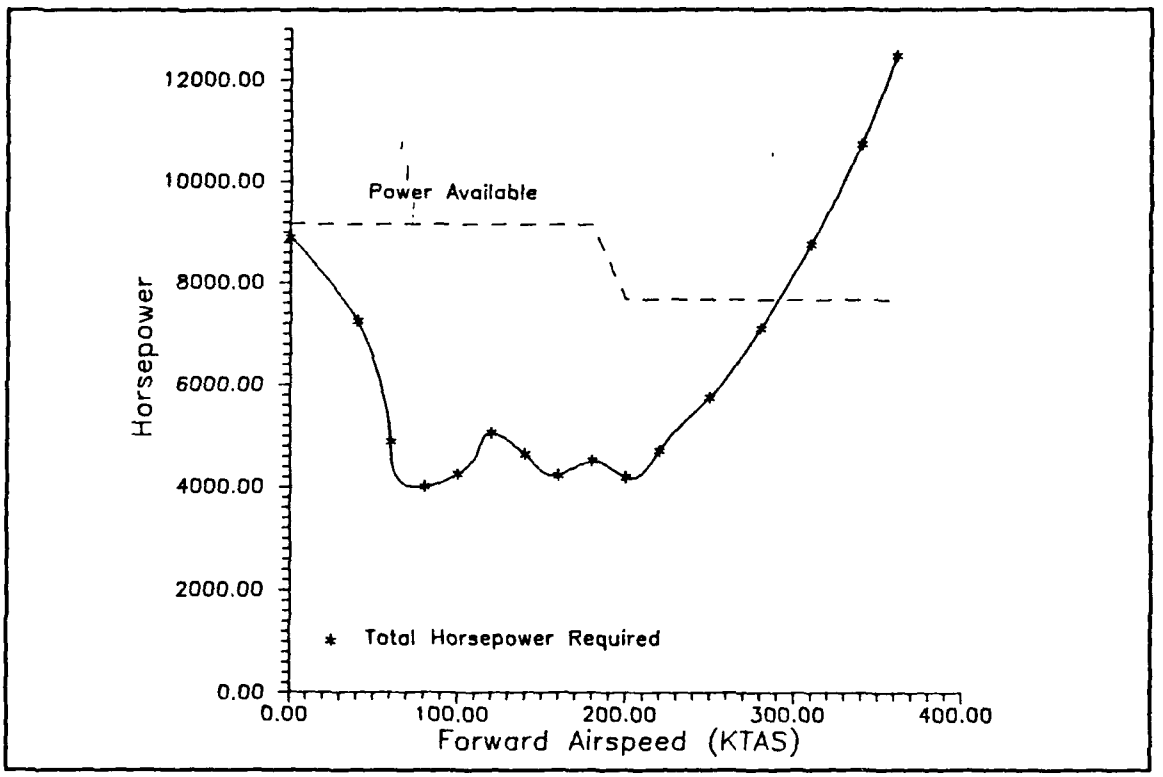

Figure 6

Power Required versus Power Available

As a final power analysis, Figure 6 displays total horsepower required along with the available horsepower. The available horsepower is the transmission rated horsepower for the current V-22 and is dependent on the engine installed (and rotor) rpm: The curve could be moved up or down if different engines were used. The drop in power available reflects the drop in rpm following transition to conventional

mode flight. The total horsepower required reflects the dual nature of the tilt rotor. At low forward airspeeds where the rotor induced power dominates, the power required curve is typical of rotary-wing behavior. At high forward airspeeds the parasite power dominates and the power required curve is typical of conventional fixed-wing behavior. In the middle ranges of airspeed there is convoluted, mixed behavior that is probably due to the effects of rotor-wing interference and transition from one mode of flight to another.

Various aspects of performance for the two baseline aircraft are presented in Table 7. Specific range is shown for best-range velocity: It is defined as the range in nautical miles per pound of fuel consumed. Specific impulse, shown for best-endurance velocity, is a comparative scale of energy consumption. It is defined as the ratio of thrust (in pounds) to fuel flow rate (in pounds of fuel per hour). Therefore, specific impulse is the hypothetical time that a given thrust generator could operate by consuming an amount of fuel equal to the generated thrust [Ref. 5, p. 4].

TABLE 7

BASELINE AIRCRAFT PERFORMANCE

Sea Level, 103 degrees F	CSAR MISSION	ASW MISSION
In Hover		
Induced Velocity (fps)	72.31	72.32
Rotor Induced Power (hp)	7177	7181
Rotor Profile Power (hp)	1143	1144
Total Horsepower Required	8880	8885
Vertical Climb, 500 fpm		
Horsepower Required	9258.9	9263.6
Forward Flight		
Best-Range Velocity (knots)	249	249
Specific Range (nm/lb of fuel)	0.0842	0.0842
Best-Endurance Velocity (knots)	195	195
Specific Impulse (hours)	2.19	2.19
L/D Ratio	8.77	8.77
Dash Velocity (knots)	290.9	290.9
Horsepower Required	7670.0	7669.9
3000 ft., 91.5 degrees F		
One Engine Inoperative		
Maximum Forward Velocity (knots)	206.9	206.9
Maximum Gross Weight (lbs)	45255	45269
Maximum Rate of Climb (fpm)	501.6	

IV. ROTOR CHARACTERISTICS

According to Johnson, "The major parameters to be selected in the preliminary design stage are the disk loading, tip speed, and solidity," [Ref. 3, p.319]. These three parameters are interrelated and highly dependent on each other. Figure 7 is a "pseudo-code" representation illustrating the algorithm used in the TR-87 DESIGN subroutine that calculates rotor characteristics.

A. DISK LOADING

Disk loading is perhaps the most important design characteristic of a rotary-wing aircraft. In fact, in the pure Momentum approach of modeling helicopter performance, disk loading is the only significant design parameter. Continuing with his discussion of rotor parameters, Johnson states the following:

> For a given gross weight, the disk loading determines the rotor radius. The disk loading is a major factor in determining the power required, particularly the induced power in hover. The disk loading also influences the rotor downwash and the autorotation descent rate. [Ref. 3, p. 319]

Because of its importance in rotor-craft design, the impact of disk loading on other design parameters will be discussed fairly extensively. The tradeoffs that occur in varying disk loading will overlap and impact on selection of other parameters.

ROTOR CHARACTERISTICS ALGORITHM

IF (fallout V_t is to be calculated) THEN
  Calculate V_t from input parameters and current value for MGW

$$V_t = \mathrm{SQRT}\{(\sigma\ \mathrm{MGW})/(2\ C_T\ R\ b\ \rho\ c)\} \qquad (1)$$

ELSE
  Use input value for V_t
ENDIF
IF (input value for disk loading set as constant) THEN
  Calculate R from DL

$$R = \mathrm{SQRT}\{\mathrm{MGW}/(2\ \pi\ \mathrm{DL})\} \qquad (2)$$

ELSE
  Use input value for radius (R) or calculate fallout value
  IF (fallout value for R to be calculated) THEN
    Calculate R from input parameters and current value for MGW

$$R = \frac{\sigma\ \mathrm{MGW}}{2\ C_T\ V_t^2\ \rho\ b\ c} \qquad (3)$$

  ELSE
    Use input value for R
  ENDIF
  Calculate DL from R

$$\mathrm{DL} = \frac{\mathrm{MGW}}{2\ \pi\ R^2} \qquad (4)$$

ENDIF
IF (fallout value for chord (c) is to be calculated) THEN
  Calculate c from other parameters and current value for MGW

$$c = \frac{\sigma\ \mathrm{MGW}}{2\ C_T\ R\ V_t^2\ \rho\ b} \qquad (5)$$

ELSE
  Calculate C_T/σ from other parameters and current value for MGW

$$C_T/\sigma = \frac{\mathrm{MGW}}{2\ R\ V_t^2 \rho\ b\ c} \qquad (6)$$

Figure 7

Rotor Pseudocode

Disk loading can be defined as the thrust-per-unit-area of the lift-generating surface. For level unaccelerated flight the total thrust is approximately equal to the gross weight of the aircraft, in which case disk loading for a rotor system can be represented algebraically as,

$$DL = \frac{\text{Gross Weight}}{\text{Area}}$$

where A is now the total disk area of the lifting rotors, or twice the area of one rotor in the case of the tilt-rotor. In TR-87, disk loading is formulated as mission gross weight (MGW) divided by total disk area, or,

$$DL = \frac{MGW}{2 \pi R^2} \qquad (4)$$

For cases where disk loading is input, the rotor radius becomes a fallout parameter calculated as,

$$R = SQRT\{MGW/(2 \pi DL)\} \qquad (2)$$

1. Historical Trends

Prior to the development of the tilt-rotor, vertical-takeoff-and-landing (VTOL) aircraft were almost exclusively represented by helicopters. Helicopters have been used successfully and extensively for VTOL applications for two reasons:

- their low energy consumption per unit of generated static thrust, and
- their relatively low downwash in hover.

The advantage of the low energy consumption is fairly obvious. Lower downwash results in less ground erosion, less damage to the aircraft and loss of pilot visibility from flying debris at unprepared landing sites, and less hazard to ground personnel operating within downwash-covered areas. In addition, downwash acting on the fuselage and wings (download) increases vertical drag in hover and climb: The result is an added requirement in power to overcome the download. Energy consumption and downwash associated with static thrust generation are both proportional to disk loading.

Stepniewski presents a figure [Ref. 5, Vol. I, Fig. 1.1] that shows a continued increase over the years (up through 1980) of disk loading in both helicopters and tilt-rotor aircraft. In 1979 Stepniewski wrote the following:

> Although historically there is a continuous trend to increase the disc loading of helicopters, it can be seen from Fig 1.1 that its current value appears to level off at $w=50$ kG/m^2 ($w=10$ psf) for medium and heavy gross-weight machines, while the value of the lighter aircraft appears to be much lower.
>
> There are only a few inputs from tilt-rotor aircraft actually flown or being developed, but they seem to indicate $w=70$ kG/m^2 ($w=14$ psf) as the upper limit of the disc loading. However, this trend reflects only relatively small aircraft, while for larger machines, as in the case of helicopters, w may increase with gross weight. In view of this and from additional design studies of large aircraft, it appears that $w = 100$ kG/m^2 ($w = 20$ psf) can be assumed as the upper limit for the tilt-rotor concept. [Ref 5, Vol. I, p. 4]

Time will tell if Stepniewski's forecast of an upper limit on disk loading for tilt-rotor aircraft was accurate. It is interesting to note that his figure of 20 psf came remarkably close to the fallout value of 19.95 and 19.96 psf for the two baseline aircraft CSAR mission for this study.

2. Disk Loading Trade-Offs

Selection of rotor diameter (and, hence, disk loading for a given gross weight) involves design trade-offs. For good hover efficiency, the rotor diameter should be large, corresponding to a low disk loading. However, the diameter should be small to minimize total aircraft weight and cost and to reduce compressibility effects due to high tip speeds. If the disk loading is too high, there will be little margin for increased loading, as may occur in maneuvering flight or due to perturbations in level flight. If the disk loading is too low, the design will be inefficient: A large rotor will be used to manage an aircraft weight that could be handled by a smaller rotor.

In addition, to develop the same thrust a small rotor must induce a higher velocity than a large rotor, resulting in two adverse effects:

- Increased ground erosion and hazard to personnel; and,
- Higher power required to overcome large vertical drag (Download) on the fuselage and wing.

In a tilt-rotor design the increase in vertical drag is even more pronounced because of the increased surface area on which the downwash is acting. The introduction of turbine engines with high power-to-weight ratios permitted designers to develop helicopters with smaller rotors (or higher disk loading). The result has been more compact aircraft that save on weight, cost, and drag; these smaller aircraft are easier to hangar and are better suited for shipboard operations.

In a conventional fixed-wing aircraft, the required thrust is only a fraction of the gross weight because the lift in forward flight is provided by the wings.

Therefore, the disk loading compromise in tilt-rotor aircraft design is even more pronounced than for helicopters. It is possible to use higher disk loading in high-speed forward flight; and this is especially desireable due to shipboard (aircraft size) constraints. However, this higher disk loading has adverse effects on hover and vertical flight capabilities due to higher power requirements, as well as loss of autorotational capability.

B. TIP SPEED

For a rotor system with a given radius and rotational speed (Ω) in radians per second, tip speed is defined as,

$$V_t = (\Omega R) \qquad (7)$$

Johnson's discussion of rotor characteristics gives an excellent explanation of the trade-offs involved in selecting tip speed:

> The rotor tip speed is selected largely as a compromise between the effects of stall and compressibility. A high tip speed increases the advancing-tip Mach number, leading to high profile power, blade loads, vibration, and noise. A low tip speed increases the angle of attack on the retreating blade until limiting profile power, control loads, and vibrations due to stall are encountered. Thus there will be only a limited range of acceptable tip speeds, which becomes smaller as the helicopter velocity increases. [Ref. 3, p. 319]

Weight of the rotor and drive systems may be minimized by designing for relatively high hover tip speed. However, increasing the tip speed beyond certain limits has adverse effects on other aspects of the aircraft's performance. Prouty states [Ref. 6, p. 91] that tip speeds greater than 750 feet per second (fps) make a rotary-wing aircraft unacceptably noisy. He gives other limits on tip speed:

- Advancing-tip compressibility (Mach number less than 0.92)
- Retreating-tip stall ($V_f/V_t = \mu$ less than 0.5, where V_f is the forward airspeed of the aircraft).

The maximum forward speed of a conventional helicopter is limited by either drag divergence on the advancing blade or blade stall on the retreating blade. In forward flight the advancing tip of the rotor experiences higher Mach numbers than the aircraft itself because the relative velocity over the blade is the sum of the tip speed plus the forward speed. Conversely, the relative velocity is lower over the retreating blade because the forward airspeed is subtracted from the tip speed.

> Because the thrust developed at any element of a blade is equal to the local lift coefficient times the local area times the local dynamic pressure, which is a function of the square of the local velocity, it may be seen that the lower velocity of the retreating blade will produce a lower thrust unless the lift coefficient is increased by increasing the angle of attack.
> [Ref 7, p.61]

In other words, unless the angle of attack on the retreating blade is increased there will be undesirable differential thrust between the two sides of the rotor. As forward velocity is increased the angle of attack required to provide balanced thrust eventually reaches the point where a condition called retreating blade stall occurs. It is this retreating blade stall that generally limits the forward speed of helicopters.

Tilt-rotor aircraft are able to achieve higher forward speeds than helicopters because of their conversion to conventional mode flight. With the rotors in the vertical plane there is no advancing or retreating blade relative to the forward flight path. Further, in forward cruise the tilt-rotor's tip speed can be (and is) reduced because the aircraft's wings are providing lift. Therefore, limits on tip speed may

not be quite as stringent for tilt-rotor aircraft as Prouty suggests for helicopters. However, noise, compressibility, and stall problems cannot be ignored completely.

C. SOLIDITY

In the Momentum theory analysis of rotor performance, the actual rotor is modeled by a solid "actuator disk" of zero thickness and area equal to that swept out by an infinite number of blades of radius, R. In this simplified analysis, the induced velocity in hover is given by the equation

$$v_h = \text{SQRT}\{T/(2\,\rho\,A)\}, \qquad (8)$$

where A is the total disk area. The (ideal) induced power required in hover is given by

$$(P_i)_{ideal} = T\,v_h$$

$$= T\,\text{SQRT}\{T/(2\,\rho\,A)\} \qquad (9)$$

The actual induced power losses will be greater (and will have to be corrected for) due to non-uniform and unsteady velocity induced by a small number of blades.

Solidity (σ) of the rotor is defined as the fraction of the actuator disk that is actually solid, or composed of blades; in other words, it is the ratio of blade area to rotor actuator disk area:

$$\sigma = \text{(area composed of blades)/(rotor disk area)}$$

$$= \frac{b\,c\,R}{\pi\,R^2}$$

$$\sigma = \frac{b\,c}{\pi\,R} \qquad (10)$$

Therefore, solidity can be thought of as a measure of how closely the actual rotor comes to the infinite-blade model. Further, for a given disk loading and tip speed, the solidity essentially determines the rotor system's Figure of Merit, or aerodynamic efficiency. See Equation (15).

As Equation (10) illustrates, solidity is a function of rotor blade area and the number of blades used for the given rotor system. Selection of both involves design trade-offs. The number of blades chosen for a rotor system should be small for low cost, low hub drag, and low hub weight. Use of less blades results in less tip vortex interference on the following blades. On the other hand, blade number should be large for low vibration level, smoother wake, and lower induced power required. For a given disk area, selection of blade number will also determine whether the blades are slender and have less torsional stiffness, or if they are stubby with higher tip losses.

In this study the effect of the number of blades was not considered. Instead, solidity was varied by changing the blade area. Prouty gives an excellent discussion of the factors that must be considered by the designer in selecting solidity. He states that:

> The optimum blade area for hovering is a low one that forces the blade elements to operate at high angles of attack and just below stall. This condition gives the highest ratio of lift to profile drag as well as the lowest blade structural weight. Unfortunately for most helicopter designs, this desireable approach cannot be fully used because high-speed maneuver requirements will dictate more blade area than is optimum for hover.
> [Ref. 6, p. 5]

In the case of a tilt-rotor, the maneuvering requirements are not as restrictive on the selection of rotor solidity because the wings are providing lift in forward flight.

However, it might still be necessary to select higher solidity than is optimum for hover in order to prevent blade flapping, since lower solidity means more slender blades for a given radius.

D. DOWNLOAD

A rotor system generates thrust by imparting downward momentum to air, from which the lift reaction of the rotor is obtained. The velocity of the downward air in hover--or induced velocity--can be calculated as

$$v_h = \text{SQRT}\{T/(2\ \rho\ A)\} \qquad (8)$$

$$= \text{SQRT}\{DL/(2\ \rho)\} \qquad (11)$$

The generation of lift results in induced power losses, as previously explained. In addition, the rotor downwash acting on the fuselage and wing produces a vertical drag force on the aircraft in hover and vertical flight. This increase in vertical drag requires an increase in rotor thrust for a given gross weight and, hence, degrades rotor performance. Download, therefore, is not really a design parameter: It is actually an effect, and is dependent on the choices made for design parameters. It is highly dependent on disk loading, fuselage vertical flat plate drag area,and--in particular for a winged helicopter or tilt rotor--on wing planform area.

A method for estimating download is contained in the U.S. Army Engineering Handbook [Ref. 8, pp.3-28]: "Based upon theory and some test data, the wing download in hover is equal approximately to one-half the disk loading times the wing area exposed to the rotor wake." Stepniewski and Keys give a more detailed

method for calculating download [Ref. 5, Vol. II, pp. 37-43] that involves calculating vertical flat plate drag areas as well as the induced velocities acting on those areas. The TR-87 subroutine that calculates download employs a variation of the method outlined in Stepniewski and Keys that was developed at NASA Ames Research Center. The algorithm, called the Magee Download Model, uses geometric data input to the program to calculate the flat plate drag area affected by downwash and multiplies it by an empirical factor derived by OARF tests on the V-22 rotor-wing combination [Ref. 4].

E. OTHER RELATED PARAMETERS

Variation of rotor characteristics forces changes in other rotor parameters. Therefore, a brief discussion of some of these parameter and their importance follows.

1. Figure of Merit

The figure of merit is a useful non-dimensional measure of the aerodynamic efficiency of a hovering rotor system. The computer code (TR-87) did not calculate or output a value for figure of merit. Further, different authors give slightly different variations of the equation for this parameter. The method chosen for this analysis was based on Johnson's approach [Ref. 3, p. 35]. Johnson defines figure of merit as the ratio of minimum possible power required to hover to actual power required to hover:

$$(P_i)_{ideal} = T\, v_h$$

$$= T\, \mathrm{SQRT}\{T/(2\, \rho\, A)\} \qquad (9)$$

$$(P_i)_{actual} = k\,(P_i)_{ideal}$$

$$= 1.15\,(P_i)_{ideal} \qquad (12)$$

$$P_o = \frac{1}{8} C_{do}\,\rho\,\sigma\,A\,V_t^3 \qquad (13)$$

$$FM = \frac{(P_i)_{ideal}}{(P)_{total}}$$

$$= \frac{(P_i)_{ideal}}{(P_i)_{ideal} + P_o} \qquad (14)$$

The factor k in Equation (12) is a loss correction factor calculated as the non-uniform inflow factor divided by the tip loss factor. These two empirical factors were entered as 1.116 and 0.97, respectively. An empirical average drag value of 0.01076 was used to calculate profile power in Equation (13). This approach involves an approximation for the actual power required to hover: losses due to the transmission, accessories, etc., are ignored. In making these calculations the thrust was rotor thrust alone: jet thrust of the engine was not considered.

Since total power required to hover is approximated by the sum of actual induced power and profile power required to hover, Equation (14) can be written as

$$FM = \frac{T\,v_h}{(P)_{total}} \qquad (15)$$

It is possible to see that a larger figure of merit corresponds to a larger thrust developed per unit horsepower input. Johnson notes [Ref. 3, p. 332] that for a

fixed disk loading the figure of merit is essentially a measure of the blade profile drag to lift.

A fairly typical value of figure of merit for modern helicopters is 0.75. The V-22 airfoils were developed in the 1980's specifically for use on the V-22 rotor system. In testing this rotor system it was found that it has a higher peak figure of merit than for typical helicopter rotors: The V-22 rotor system has a peak figure of merit of 0.81 at a blade loading of 0.13 [Ref. 4, p. 13]. Reasons for this higher figure of merit include the high disk loading of the system and the extremely high amount of twist (- 47.5 degrees) employed in the blades. At high disk loading the profile power is small compared to the total power; whereas the high twist provides fairly uniform circulation distribution along the blade span at high coefficients of thrust.

2. Blade Loading

Another extremely important non-dimensional parameter is blade loading (C_T/σ). Blade loading is defined as the coefficient of thrust (C_T) divided by solidity, where,

$$C_T = \frac{T}{A \rho V_t^2}$$

$$= \frac{DL}{\rho V_t^2} \qquad (16)$$

$$C_T/\sigma = \frac{DL}{\sigma \rho V_t^2} \qquad (17)$$

In the actuator disk model the thrust is spread evenly over the entire disk area. As seen by Equation (17), the actual loading of the individual blades is related to disk loading and solidity. If disk loading is increased, blade loading increases; if solidity is increased, blade loading decreases. In his section entitled "Main Rotor Design" [Ref. 6, p. 92] Prouty shows a plot of Figure of Merit vs. Blade Loading. From that figure it appears that a desireable value for blade loading would be in the broad area of maxima, or roughly 0.08 to 0.14. Equation (9) can be written as,

$$(P_i)_{ideal} = T\ SQRT\{DL/(2\ \rho)\} \qquad (18)$$

Then it can be seen from Equation (14) that figure of merit is low for low blade loading because of reduced disk loading. At higher values of blade loading retreating blade stall results in increased profile drag and, hence, lower figure of merit.

3. Power Loading.

A direct measure of aerodynamic efficiency and energy consumption is provided by power loading (PL): High power loading corresponds to high efficiency and low energy consumption for a given thrust. Power loading can be defined as the lift generated per unit power input. Since lift is approximately equal to weight,

$$PL = \frac{MGW}{P} \qquad (19)$$

In hover, thrust equals weight. From basic momentum theory, expressions for thrust and induced power in hover can be derived from Equations (4) and (9). Algebraic manipulation leads to the following result:

$$\frac{T}{P_i} = \frac{f(\rho)}{SQRT(DL)} , \qquad (20)$$

where $f(\rho)$ is a function of density. From Equation (20) it can be seen that power loading decreases as disk loading increases.

V. AIRCRAFT CHARACTERISTICS

So far this study has been discussed from a purely rotary-wing type of analysis. The emphasis on rotary-wing performance is justifiable because the hover performance of a tilt-rotor aircraft is probably the most crucial and constraining aspect of its overall design. One has only to look at the power required curves in Section III to see that this is true.

However, sizing of the aircraft for forward flight performance is also important. The first step in conventional aircraft design is estimating the mission gross weight. After the gross weight has been determined, sizing the aircraft is largely a matter of determining wing loading as a function of thrust-to-weight ratio and wing lift coefficients to meet various requirements. In a tilt-rotor design the choice of the wing impacts both the forward flight performance and the rotary-wing performance. Note that the thrust-to-weight ratio normally should be considered concurrently with wing loading. Although parameters from the V-22 engines were input in the data decks, it was not desirable to restrict the analysis to a specific engine rating.

A. WING LOADING

Wing loading can be defined as the amount of weight supported (or lifted) by a given wing area. In most aircraft design text books the wing loading of an aircraft is generally given as its take-off weight (or mission gross weight) divided by total wing planform area,

$$WL = \frac{MGW}{S} \qquad (21)$$

Roskam states,

> From these data it usually follows that the combination of the highest possible wing loading and the lowest possible thrust loading (or power loading) which still meets all performance requirements results in an airplane with the lowest weight and the lowest cost. [Ref 9, Part 1, p.89]

In his sections on sizing aircraft, Roskam shows how required wing loading is calculated for various requirements such as stall speed, take-off distance, landing distance, climb rate or gradient, maneuvering requirements, and cruise speed. For example, in his section on "Sizing to Stall Speed Requirements" he shows the following:

> The power-off stall speed of an airplane may be determined from:

$$V_s = \{2(W/S)/\rho\ C_{L\ max}\}^{0.5} \qquad (3.1)$$

> By specifying a maximum allowable stall speed at some altitude, Eqn. (3.1) defines a maximum allowable wing loading W/S for a given value of $C_{L\ max}$. [Ref.9, part I, p.90]

In another volume of his series of books on aircraft design Roskam states that

> Wing size or wing loading primarily affects the following characteristics:
> 1. Take-off/landing field length
> 2. Cruise performance (L/D)
> 3. Ride through turbulence
> 4. Weight
>
> [Ref. 9, part III, p. 165)]

Note that for vertical-take-off-and-landing tilt-rotor aircraft the field length is not applicable, but for short-take-off-and-landing performance on land-based airfields field length could be a consideration. Roskam goes on to show the following:

- low wing loading is preferable to achieve short field lengths
- high wing loading is needed to achieve cruise flight close to (L/D)max
- high wing loading is preferable for "ride quality"
- high wing loading is preferable for keeping overall weight down.

He shows a typical range of wing loading for military patrol, bomb, and transport airplanes as 70 to 120 psf.

Since field length is generally not a significant factor in tilt-rotor performance, it is readily apparent that high wing loading is desireable from the viewpoint of forward flight performance. In addition, higher wing loading equates to a smaller wing planform area for a given gross weight. Therefore, higher wing loading is preferable from the viewpoint of rotary-wing performance as well. A smaller wing planform area will result in lower power penalties due to download and vertical drag in hover and vertical climb.

B. WING THICKNESS RATIO

To paraphrase Roskam [Ref. 9, Part III, p.11], wing thickness ratio primarily affects drag, weight, maximum lift, and fuel volume. The effect on drag is fairly easy to visualize: A thick wing (corresponding to a high value of wing thickness ratio) will result in increased drag in forward flight. The effect on weight is not as readily apparent. Roskam states, "Increased wing thickness means decreased wing weight since both bending and torsional stiffness increase with increasing thickness" [Ref. 9, part III, p. 187]. In his second volume Roskam presents a figure (not reproduced here) showing the effect of wing thickness ratio on maximum lift

coefficients for various symmetric and cambered airfoils [Ref 9, part II, p. 119]. For all the airfoils shown, the maximum lift coefficient increased with thickness up to values of 12 to 14 percent and then started decreasing again. Finally, Roskam comments succinctly that "increased thickness translates into greater fuel volume" [Ref. 9, part III, p. 187] for a wet-wing aircraft.

In a tilt-rotor aircraft, selection of wing thickness ratio is largely a trade-off between drag and aeroelastic stability. Structurally, the tilt rotor requires a larger wing thickness than a conventional fixed-wing aircraft in order to support the combined weight of the rotor blades, pylons, engines, and conversion mechanisms located at the wing tips.

VI. VARIATION OF DISK LOADING

The fallout baseline disk loading of the CSAR mission was 19.95 psf; and the ASW input deck was modified to yield a comparable value for disk loading of 19.96 psf. The desired range for varying disk loading was determined to be 10 to 35 psf; however, for the constraints discussed in the next section, the computer code was unable to perform for values below 15 psf without returning a lower value of disk loading than was input.

A. METHOD OF VARYING DISK LOADING

In order to study the effect of disk loading variation, the desired value was entered in the input deck as a constraint. Blade loading was also fixed. The rotor diameter, hover tip speed, and solidity were among the fallout parameters. The aircraft geometry was input: The data deck was encoded with the fuselage width at the rotors, the fuselage-rotor-blade clearance, the size of the rotor spinners and the rotor pylons, and the fact that the pylons were located at the wing tips. The wing chord was fixed at the baseline value; but the wing span varied with the rotor radius to maintain the given geometry.

The analysis was actually done in two separate computer runs. After the first set of runs, it was noted that hover tip speed varied significantly over the range of disk loading. However, the program was not designed to allow cruise tip speed to vary. Therefore, a second set of computer runs was performed with the cruise tip

speeds input as 84 percent of the hover tip speeds from the first set of runs: This percentage corresponds to that for the V-22 rotor system.

B. RESULTS OF DISK LOADING VARIATION

The results of varying disk loading will largely be presented in the form of graphs of selected parameters plotted against disk loading. Figure 8 is a legend of symbols for these graphs (and for the graphs in the sections to follow) used to distinguish the data from the two mission profiles studied. Discussion of the variation of disk loading (and of the other parameters to follow) can be simplified by the following arbitrary convention: Trends will be noted in term of increasing the independent variable.

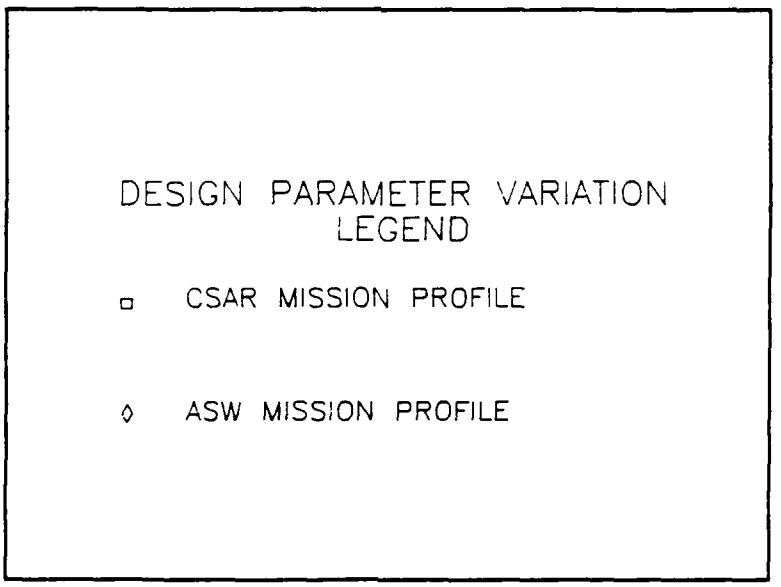

Figure 8

Legend for Graphs

1. Size and Rotor Characteristics

Aircraft designers look critically at gross weights for proposed aircraft designs because weight is almost directly related to the total aircraft cost. In addition, increasing gross weight places limitations on aircraft usage in terms of flight deck and runway weight-bearing capacities. As Figure 9 shows, increased

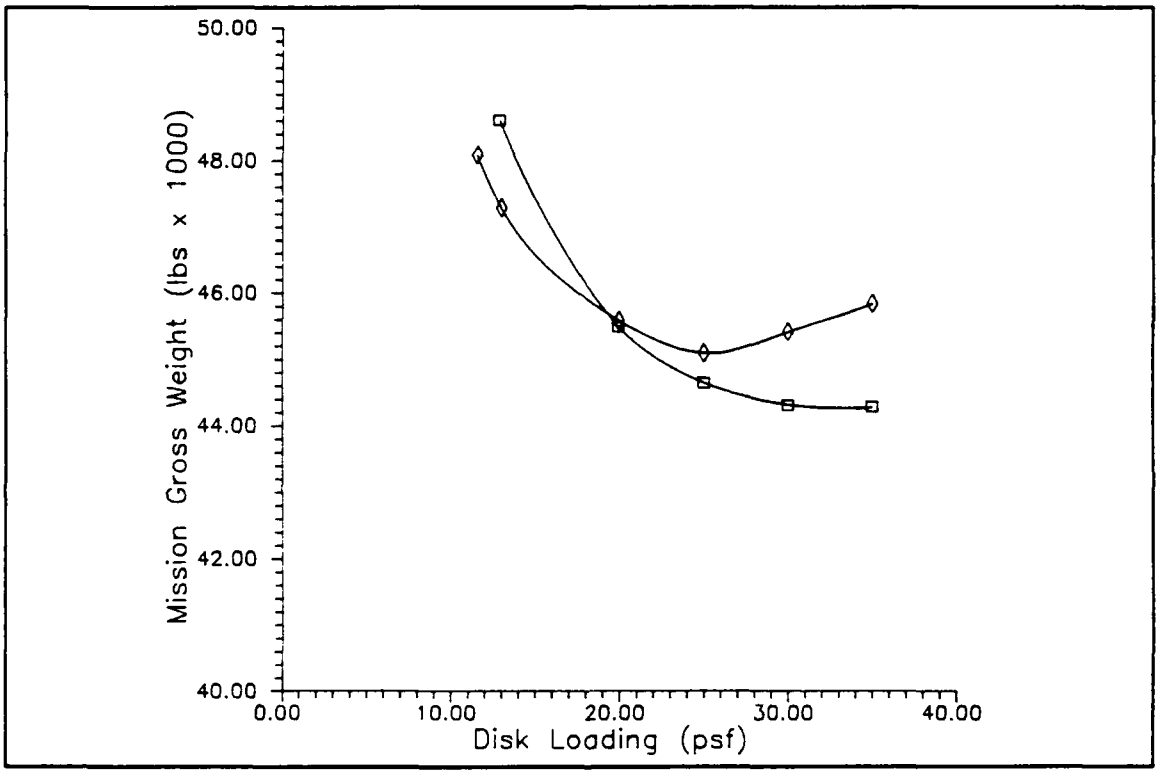

Figure 9

Mission Gross Weight
Versus Disk Loading

disk loading had a favorable impact on aircraft mission gross weight. The decrease in mission gross weight is largely due to a decrease in rotor diameter. Recall that disk loading is defined as the thrust-per-unit-area of the rotors. By definition rotor

diameter decreases (for a given thrust level) as disk loading increases, as shown in Figure 10.

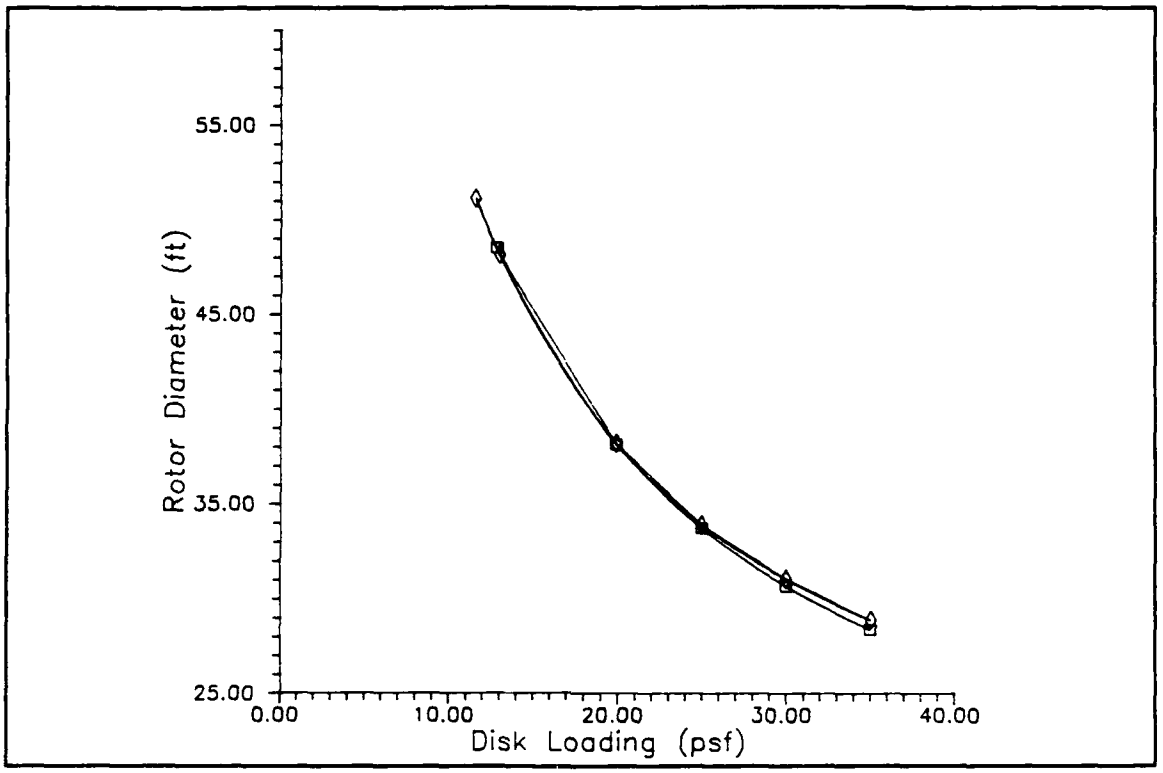

Figure 10

Rotor Diameter
Versus Disk Loading

From Equation (7) it can be seen that, for a given rotor rotation rate, tip speed is proportional to the rotor radius. Equation (1) shows that tip speed is also a function of blade chord, blade loading, and gross weight of the aircraft. For this analysis blade loading was held constant. It has already been shown that rotor radius and mission gross weight decreased as disk loading increased. In addition, the computer output reflected that blade chord also decreased. The net effect was

the decrease in tip speed shown in Figure 11. The decrease in mission gross weight initially dominated the behavior, leading to a decrease in tip speed. Over the range of disk loading studied the CSAR data continued to decline; but the decrease appeared to be flattening out at the higher end of the range. Note that the ASW data reached a minimum at a disk loading of approximately 25 psf; the subsequent increase in tip speed indicates that the effect of the rotor and chord decreases began to have more impact than the trends in mission gross weight.

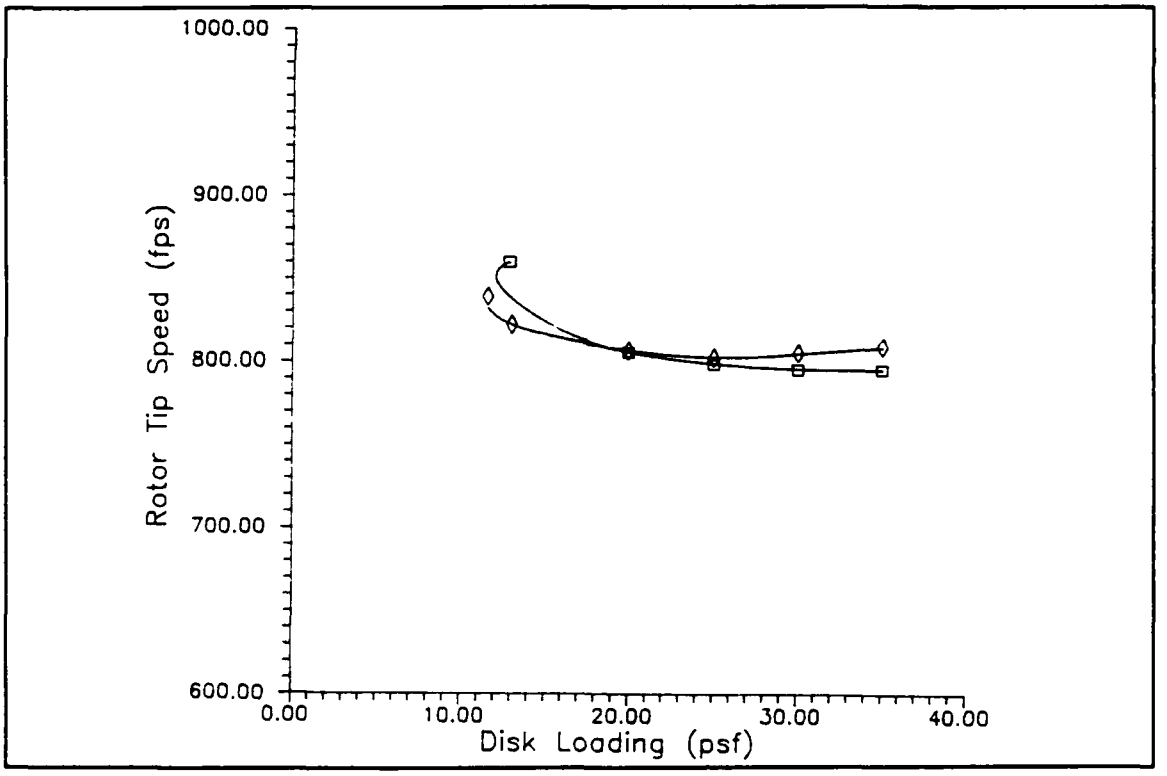

Figure 11

Tip Speed
Versus Disk Loading

Figure 12 shows variation in rotor solidity with disk loading. From Equation (10) it can be seen that the reason for the increase in solidity was the decrease in rotor radius. Further, for a given thrust and tip speed, a rotor will tend to have about the same blade area, regardless of rotor diameter. Therefore for large disk loading there will be a small disk area, low aspect ratio, and high solidity.

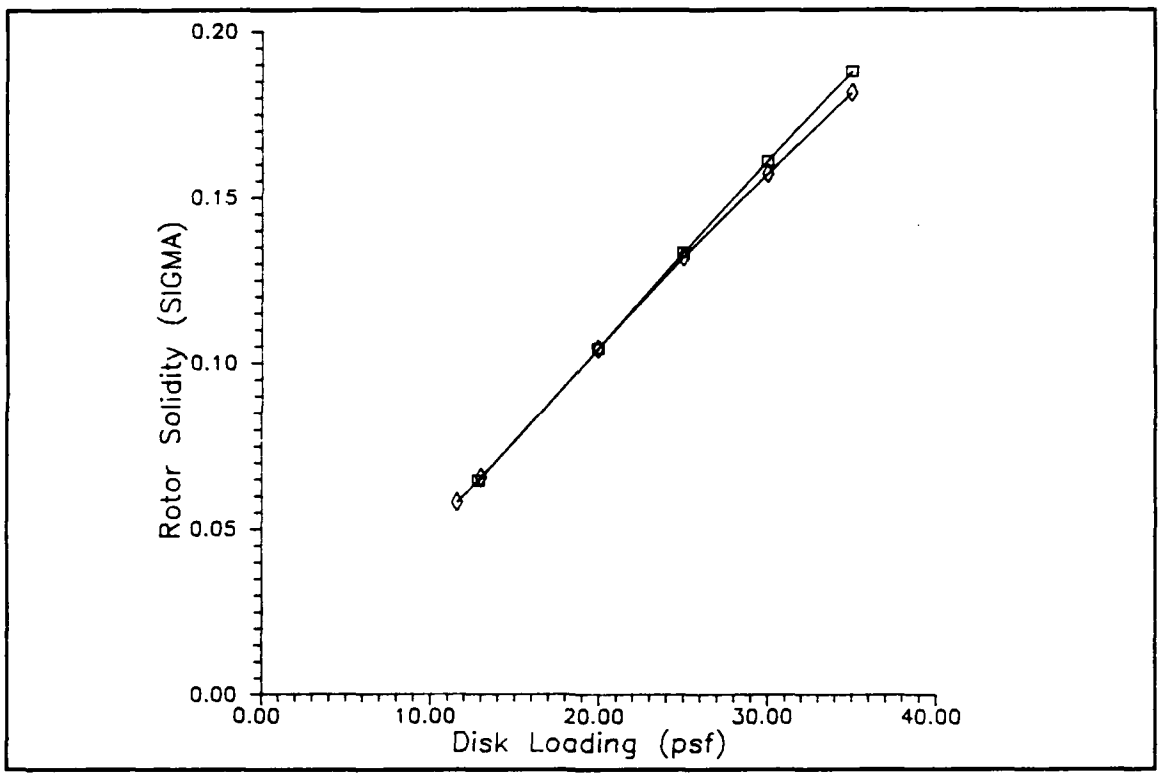

Figure 12

Rotor Solidity
Versus Disk Loading

Recall that hover-induced velocity increases with disk loading, as shown in Figure 13. As a direct result of the increased downwash impinging on the wings

and fuselage, the download percentage increased also, as shown in Figure 14. Because of the relationship in Equation (9), the substantial increase in induced

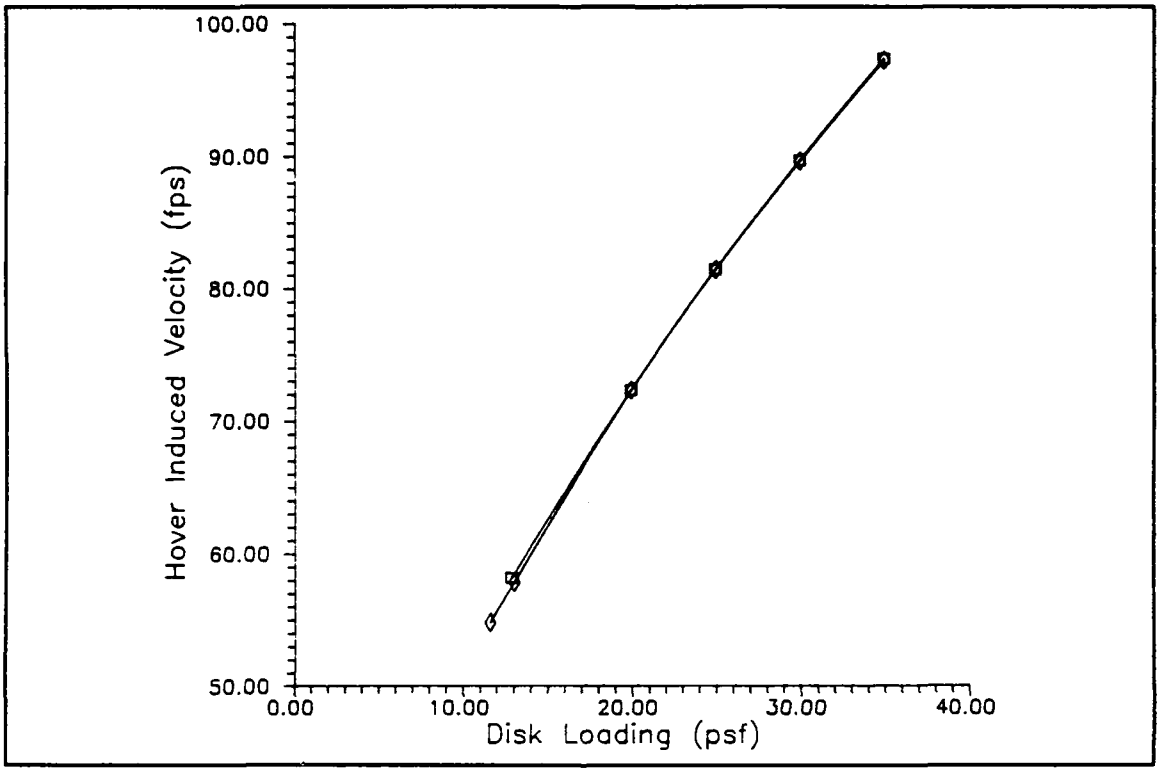

Figure 13

Induced Velocity
Versus Disk Loading

velocity also resulted in the significant increase in induced power shown in Figure 15. Rotor profile power also increased (slightly) because of the relationship in Equation (13): Solidity increased fairly substantially compared to the relatively flat trends in tip speed. The net effect on total power required for hover was essentially a result of the changes in rotor induced power.

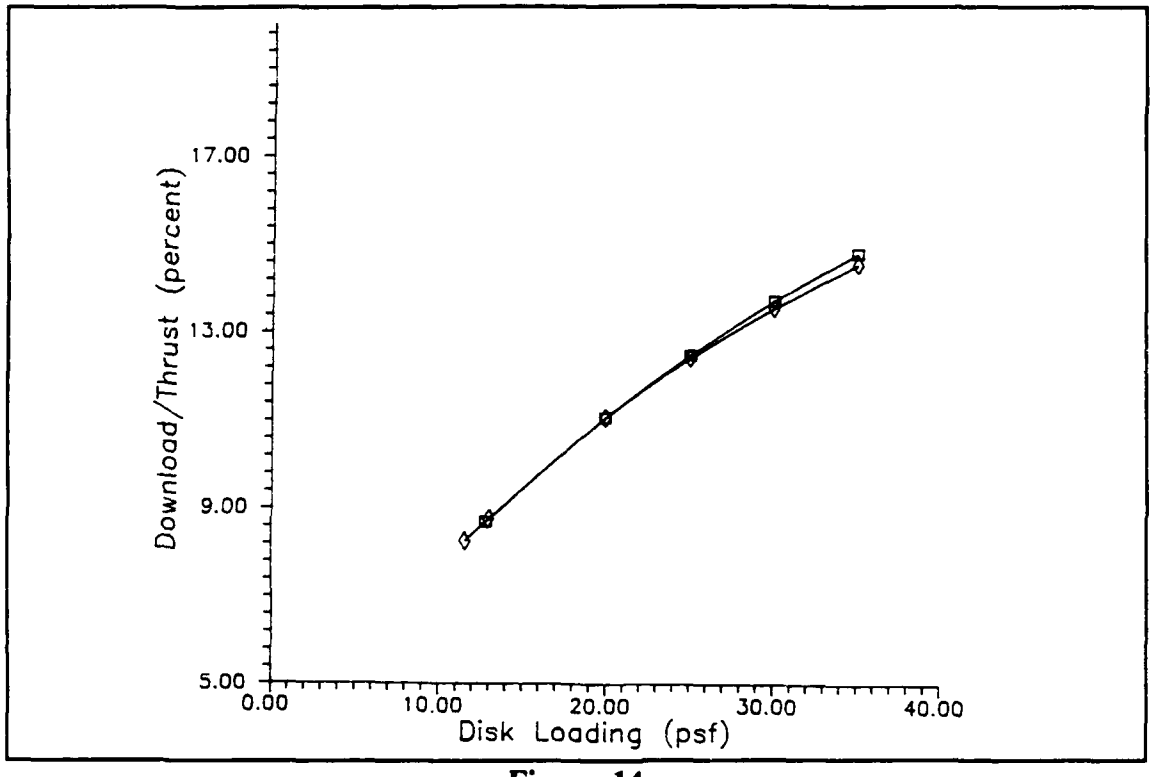

Figure 14

Download
Versus Disk Loading

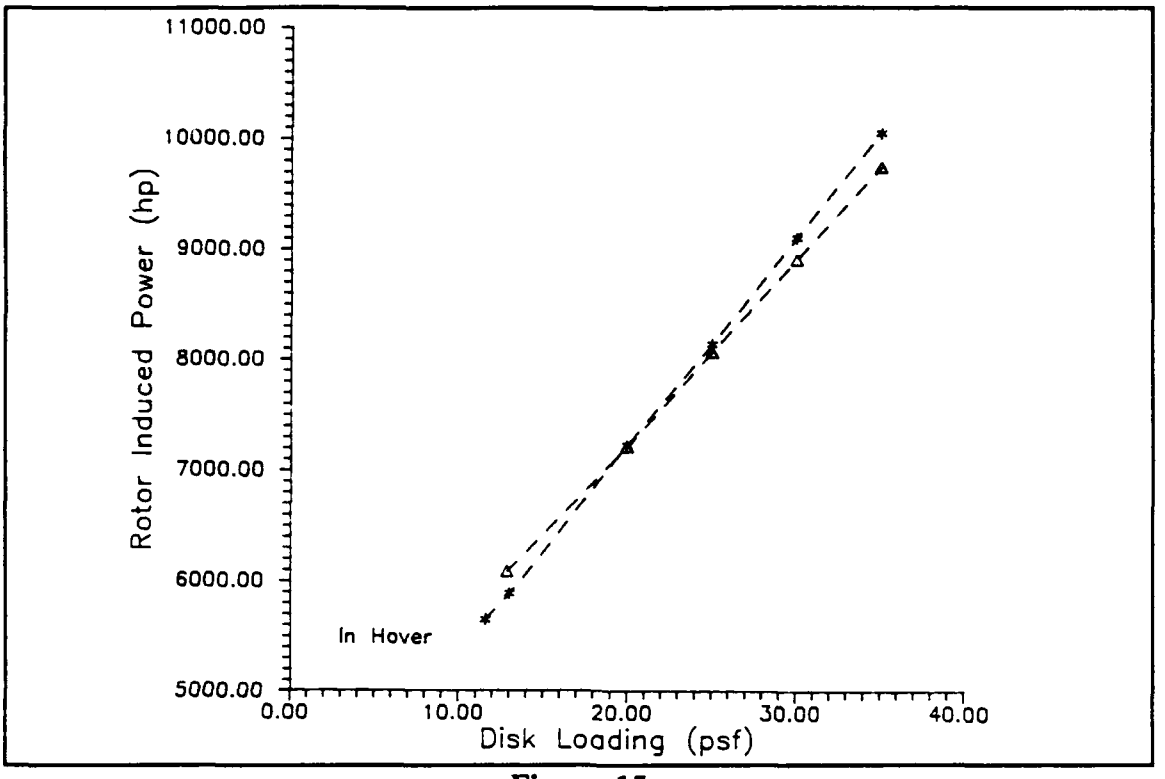

Figure 15

Induced Power
Versus Disk Loading

Figure of merit increased (from 0.712 to 0.806) because induced power increased significantly while rotor profile power remained fairly constant. This slight increase corresponds to the phenomenon noted by Felker:

> The high disc loading and high twist of these rotors contribute to their high peak figures of merit. At high disc loadings the profile power is small compared to the total power. The highly twisted blades allow a fairly uniform circulation distribution along the blade span at high thrust coefficients, and thereby allow efficient operation. [Ref. 6, p. 13]

Although hover efficiency increased, Figure 16 confirms the fact stated in the discussion of rotor characteristics that power loading decreases as disk loading increases.

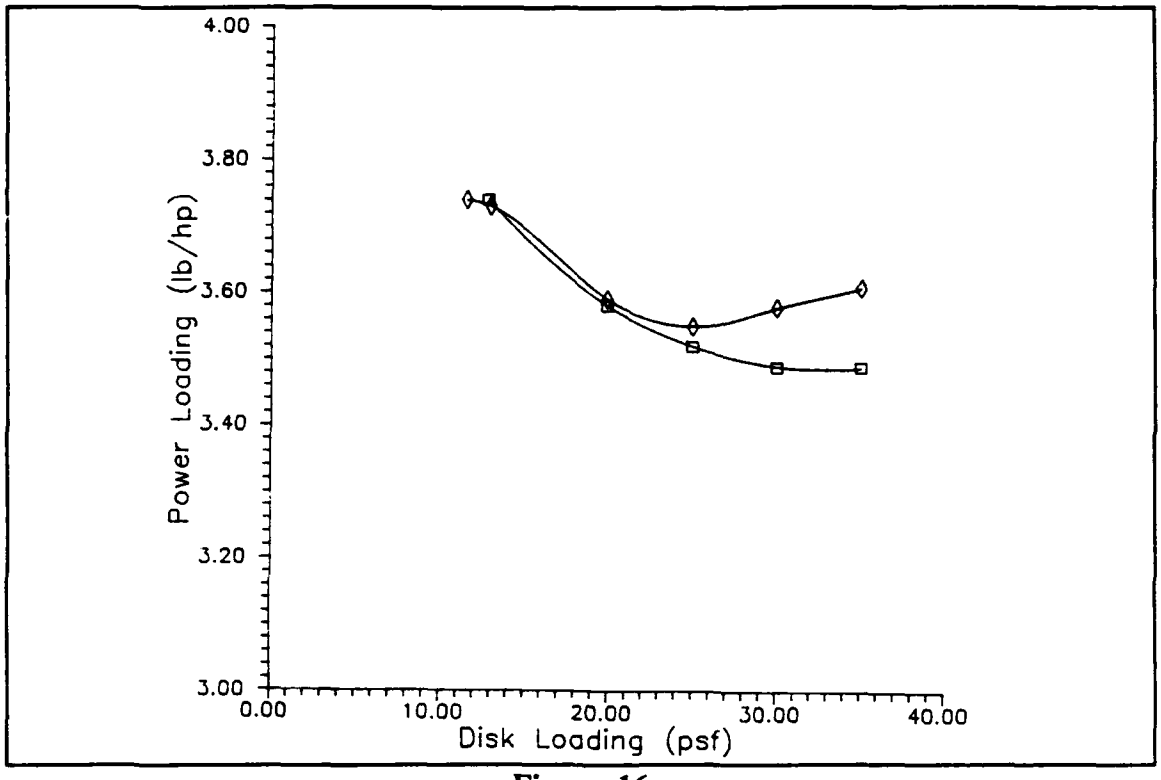

Figure 16

Power Loading
Versus Disk Loading

2. Aircraft Characteristics

Figure 17 shows the effect of increased disk loading on wing loading. This was due to the geometric relationship between the rotor radius and wing span. The input decks were encoded so that the clearance between prop-rotor tips and the fuselage in forward flight was a given value; further, the rotor assembly was fixed at the end of the wings. Therefore, the wing span decreased as the rotor radius decreased; whereas the wing chord was held constant. As a result, wing loading increased because of the decrease in wing planform area.

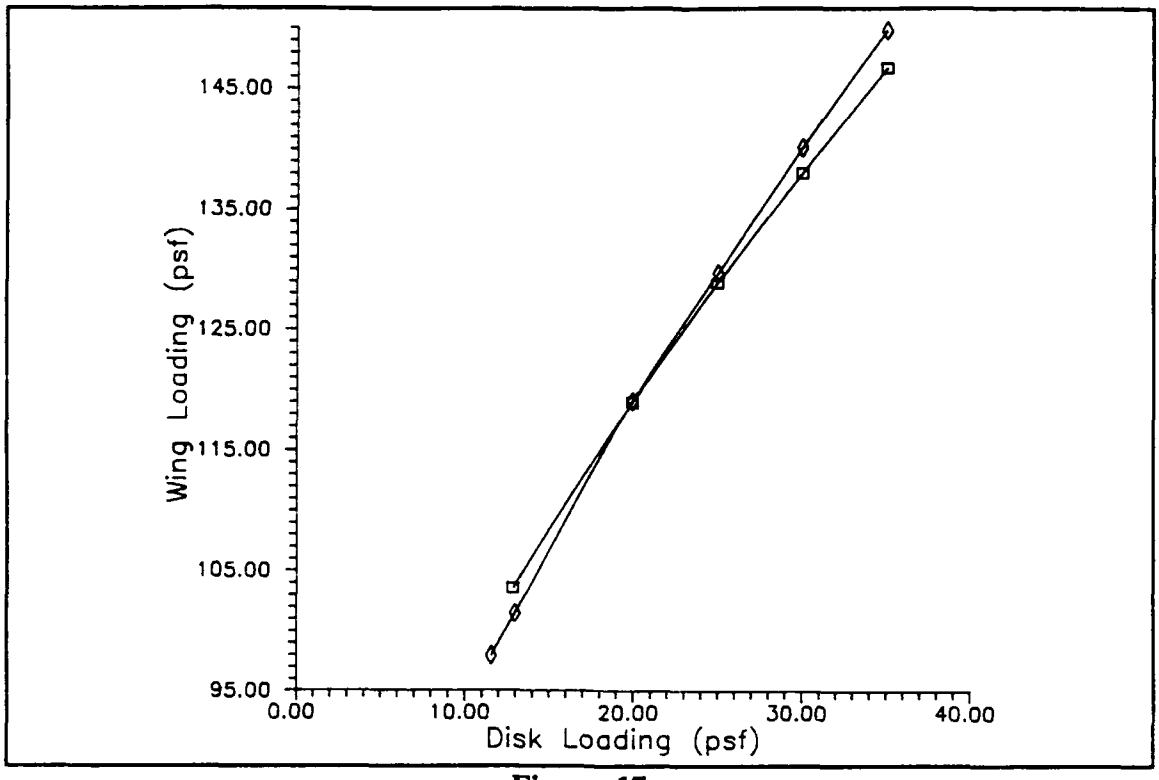

Figure 17

Wing Loading
Versus Disk Loading

The reductions in wing aspect ratio also resulted in a loss of lift in forward flight, as seen in Figure 18. In addition, it is possible that the increased prop-rotor solidity led to increased drag, which would also have contributed to the decrease in L/D ratio. Note in Figure 19 that drag penalties became prominent at a disk loading of approximately 20 psf; beyond that value dash velocity began decreasing.

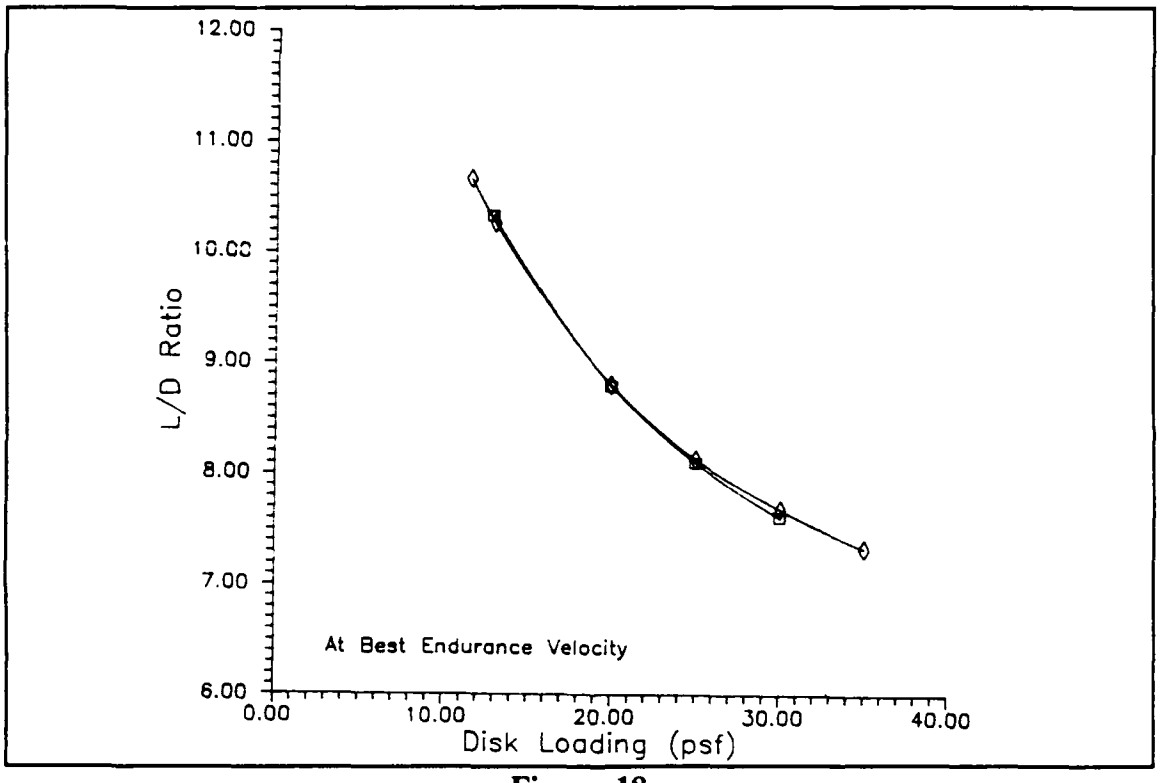

Figure 18

L/D Ratio
Versus Disk Loading

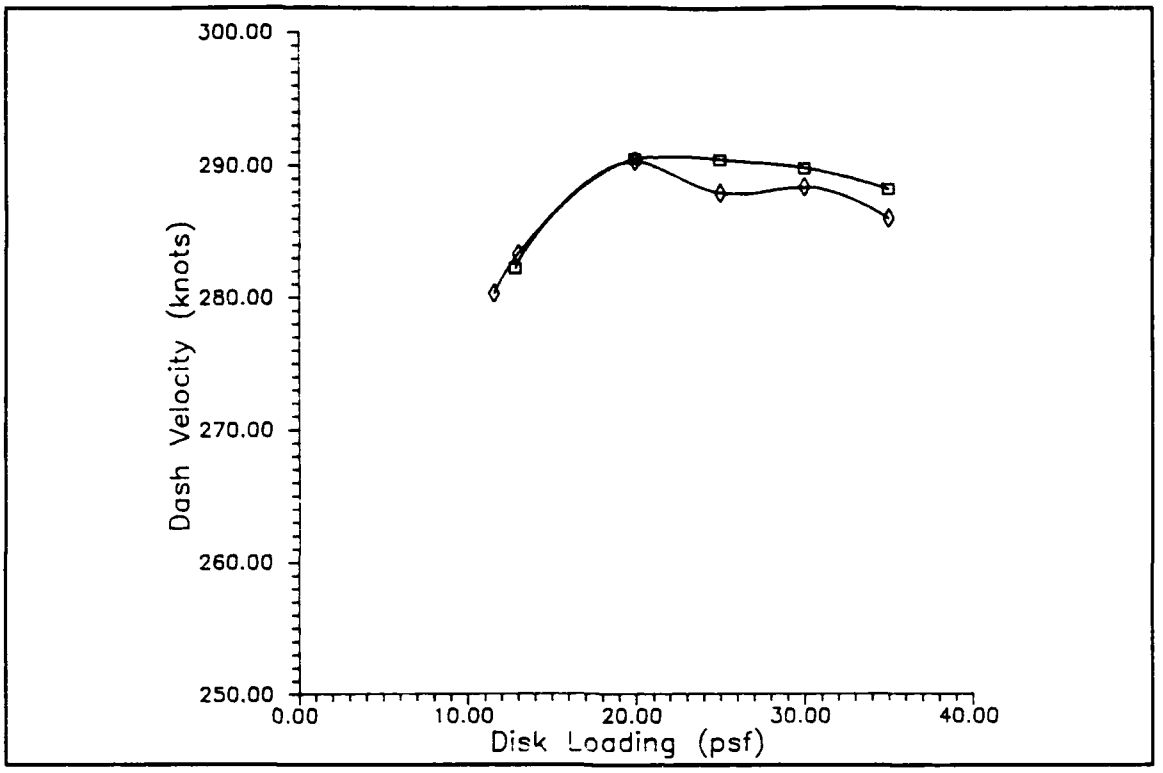

Figure 19

Dash Velocity
Versus Disk Loading

3. One-Engine-Inoperative (OEI) Performance

OEI performance for a multi-engine aircraft is always important in terms of safety, especially for an aircraft which operates in hostile territory or around a ship. For that reason, predictions of the impact of design parameter variation on tilt-rotor OEI performance are presented in Figures 20 and 21. Note that for values of disk loading less than the baseline value the gross weight that can be supported with one engine is less than the mission gross weight. On the other hand, values of disk loading above approximately 28 psf resulted in loss of vertical flight capability. In

addition, in the event of total engine failure, autorotational capability would decrease with increased disk loading, as would glide capability due to reduced wing area.

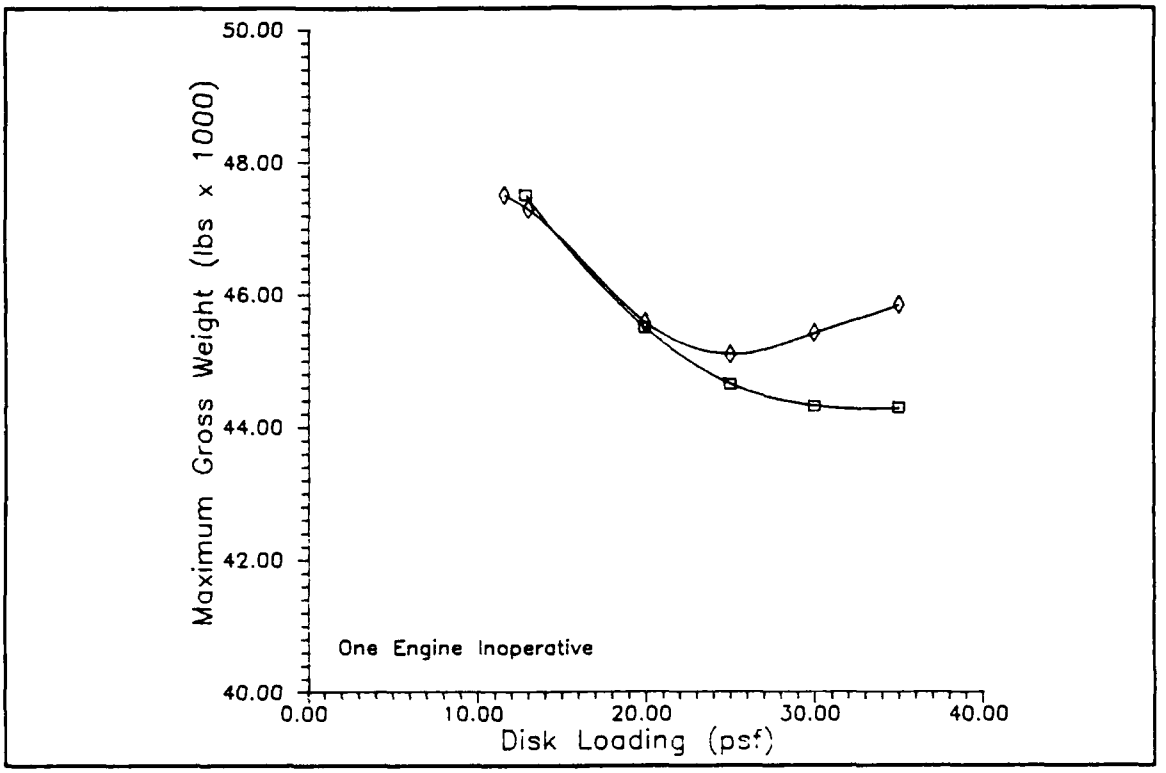

Figure 20

OEI Gross Weight
Versus Disk Loading

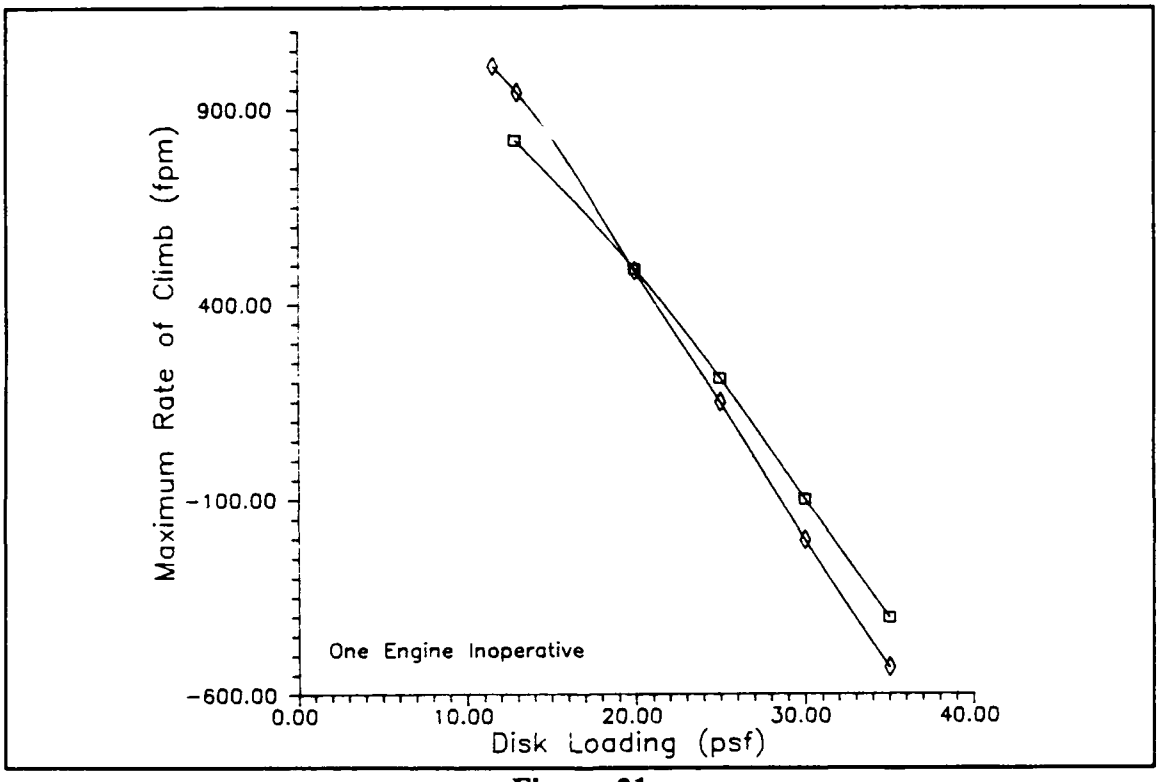

Figure 21

OEI Climb Rate
Versus Disk Loading

VII. VARIATION OF TIP SPEED

The design tip speeds for the V-22 Osprey are 790 fps and 662 fps for hover and cruise, respectively. That baseline value of cruise tip speed is roughly 84 percent of the baseline hover tip speed. It was decided in advance to vary the hover tip speed over a range of 725 to 850 fps with cruise tip speed held constant at 662 fps. In addition, computer runs were also made to analyze the effect of cruise tip speed as a percentage of baseline hover tip speed. The baseline value of 790 fps was held constant for values of cruise tip speed corresponding to 75, 80, and 85 percent of the hover value.

A. METHOD OF VARYING TIP SPEED

As hover tip speed was varied over the selected range, disk loading, blade loading, and cruise tip speed were held constant at their baseline values except for the cases in which cruise tip speed was varied: In those runs, hover tip speed was fixed at 790 fps. Blade radius and chord were both among the fallout data.

B. RESULTS OF TIP SPEED VARIATION

As was done for disk loading variation, the results of varying tip speed are presented largely in graphical form. Wherever possible the scales used on the graphs in this section and the ones to follow were chosen in order to allow comparison with the graphs in Section VI. In cases where there was no significant change in a parameter, the discussion will not be accompanied by a graph. Look at Figure 8 for a legend of symbols used.

1. Size and Rotor Characteristics

Although rotor radius was allowed to vary, there was essentially no variation from the baseline value because the disk loading was fixed. Over the range of tip speed selected for study the radius decreased from 38.3 to 38.13 feet. Note from Figure 22 that the insignificant decrease in rotor radius contributed to a correspondingly small decrease in mission gross weight.

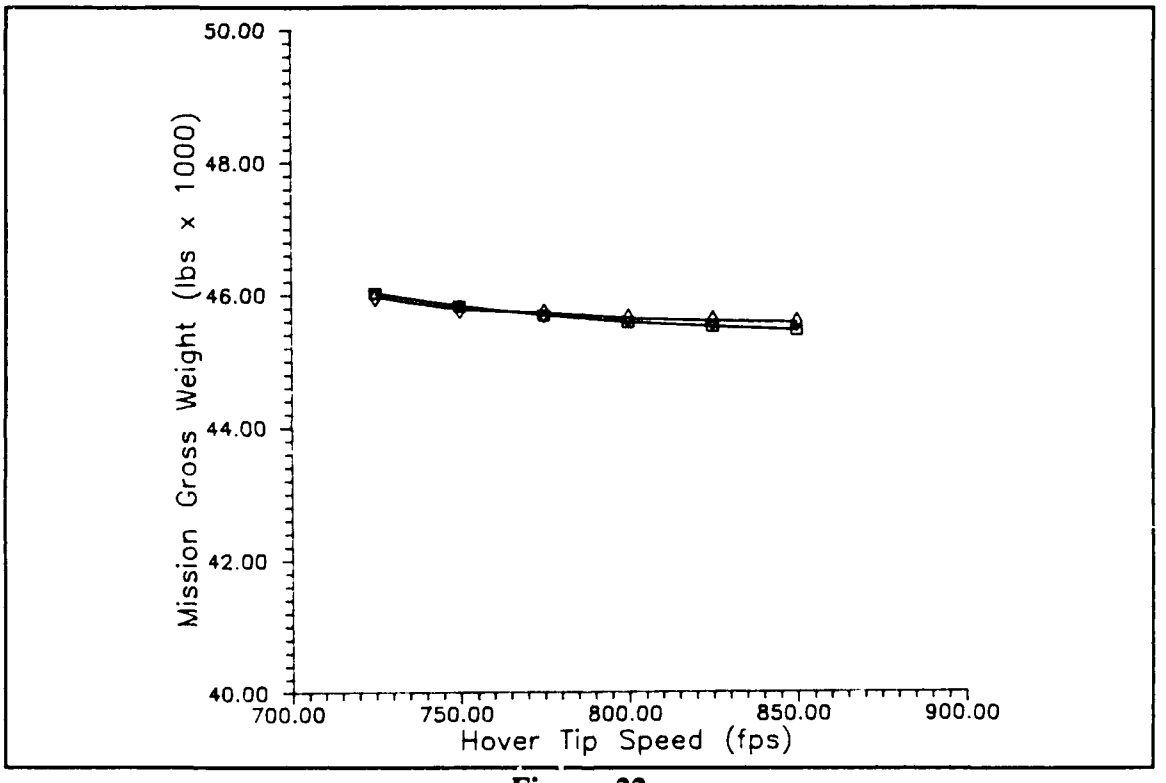

Figure 22

Mission Gross Weight
Versus Hover Tip Speed

Blade chord also decreased as tip speed increased, from 2.59 to 1.88 feet. Solidity is proportional to the ratio of blade chord to rotor radius. Therefore, as seen in Figure 23, solidity decreased.

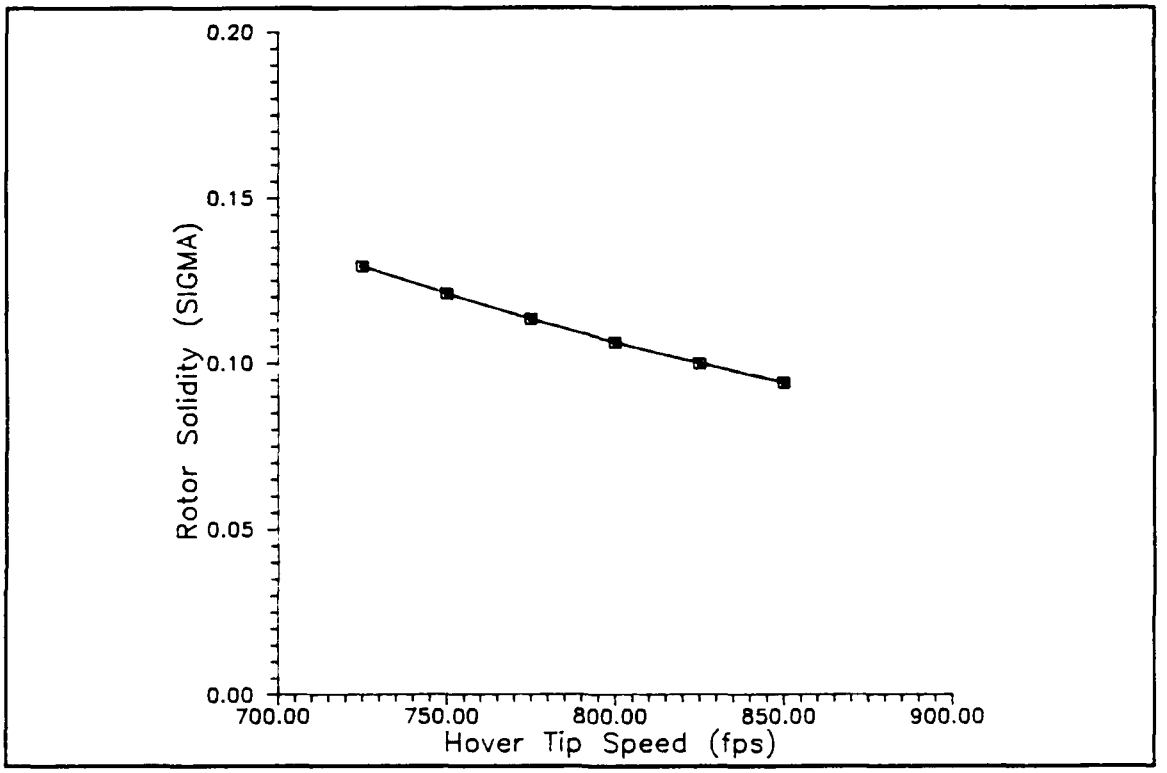

Figure 23

Rotor Solidity
Versus Hover Tip Speed

Equation (11) shows that rotor induced power is inversely proportional to rotor radius, but is directly proportional to thrust (or mission gross weight) to the power of 1.5. Therefore, induced power understandably decreased from 7287 to 7222 horsepower. Profile power increased, on the other hand, as seen in Figure 24.

This increase can be explained by the fact that, while profile power is proportional to the solidity and the square of the rotor radius, it varies as the cube of tip speed. The increase in tip speed therefore led to an increase in profile power; but the increase was small due to the decrease in both solidity and rotor radius. The effects on induced and profile power offset each other; there was virtually no variation in total power required to hover.

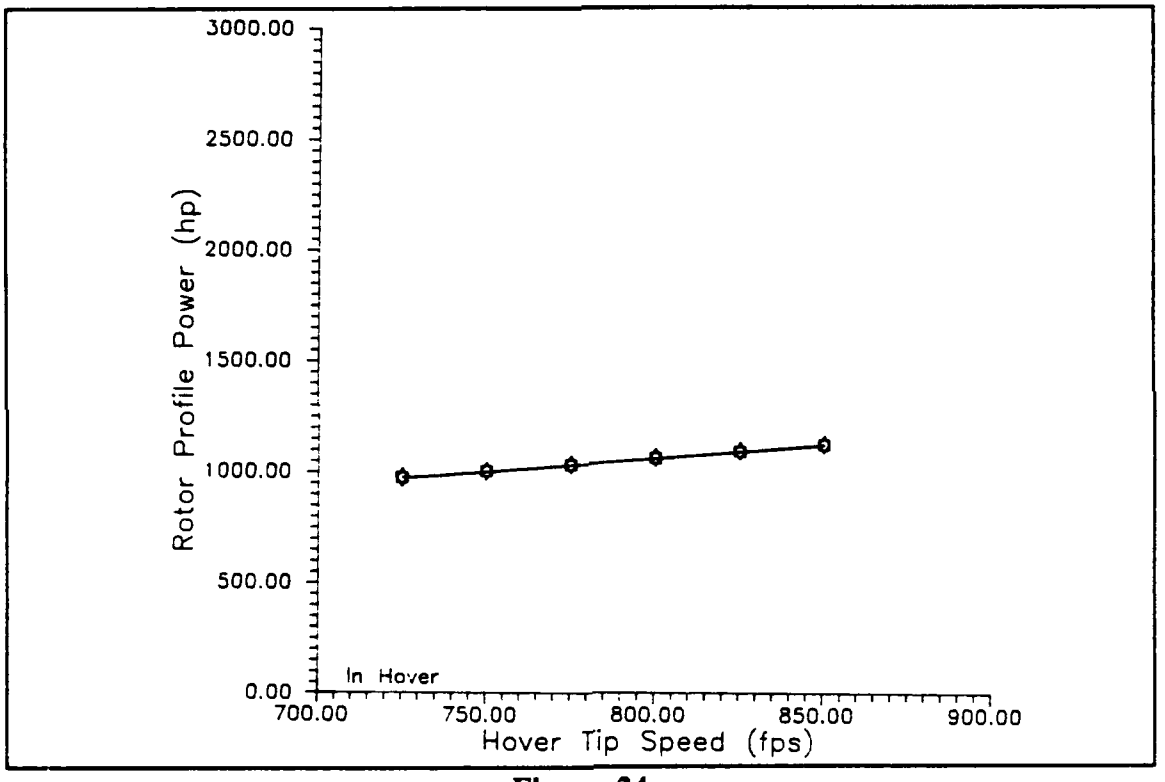

Figure 24

Profile Power
Versus Hover Tip Speed

2. Aircraft Characteristics

The variation of hover tip speed had little to no effect on aircraft characteristics. As it turned out, the variation of cruise tip speed had little effect, either. Wing loading, for example, increased by less than 10 psf. The only effect worth noting was the increase in dash velocity seen in Figure 25. Neither hover or tip speed variation had a significant impact on OEI performance.

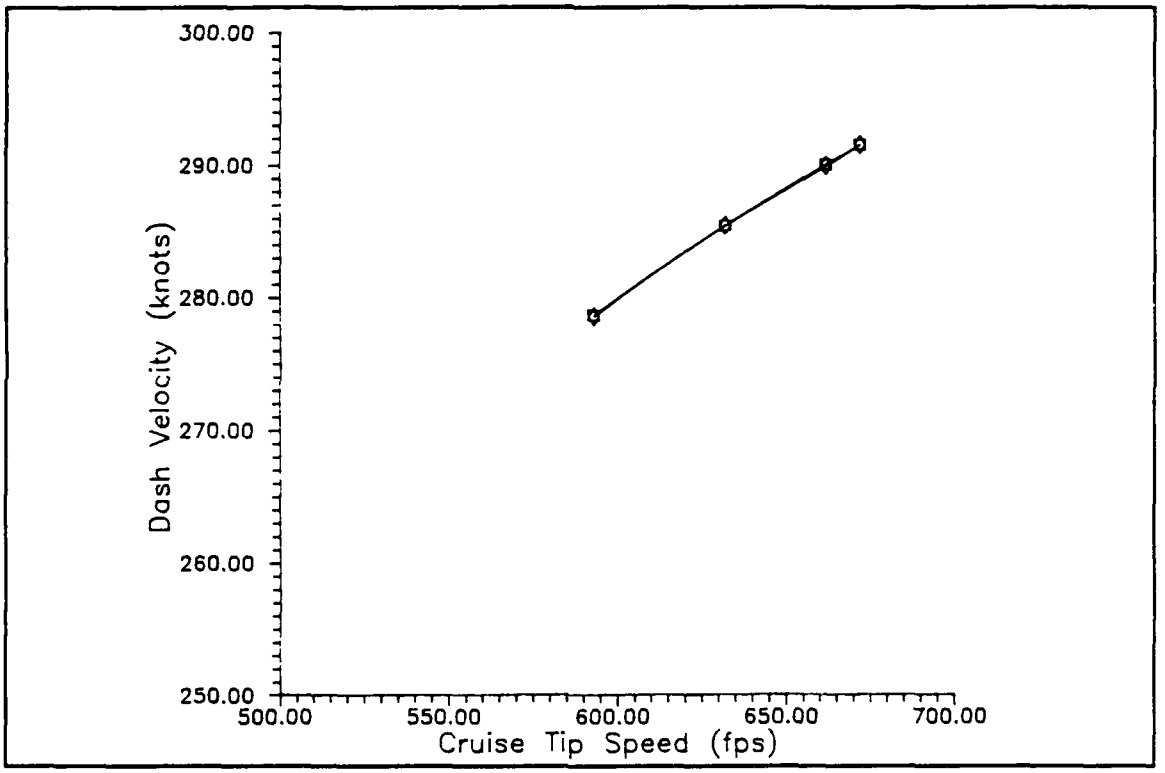

Figure 25

Dash Velocity
Versus Cruise Tip Speed

VIII. VARIATION OF SOLIDITY

The solidity for the baseline aircraft was 0.105. For this study solidity was varied over a range of 0.08 to 0.15.

A. METHOD OF VARYING SOLIDITY

For a given number of blades per rotor, solidity is a function of rotor radius and blade chord. For this study, solidity was varied by varying the rotor chord from 1.59 to 2.99 feet, with the rotor radius held constant at the baseline value.

B. RESULTS OF VARYING SOLIDITY

See Figure 8 for a legend of symbols used in the graphs presented in this section.

1. Size and Rotor Characteristics

Because the rotor radius was held fixed, disk loading increased by less than one psf as solidity was increased over the range studied. The increase in mission gross weight in Figure 26 can be partially explained by the increase in rotor blade area. Another explanation for the weight increase can be extrapolated from Equation (1) and Figure 27. What is not apparent, however, is why rotor tip speed decreased: Equation (7) would lead one to believe that tip speed should not have varied unless rotor rpm changed. Indeed, the computer program predicted that rotor rpm decreased from 463 to 343.

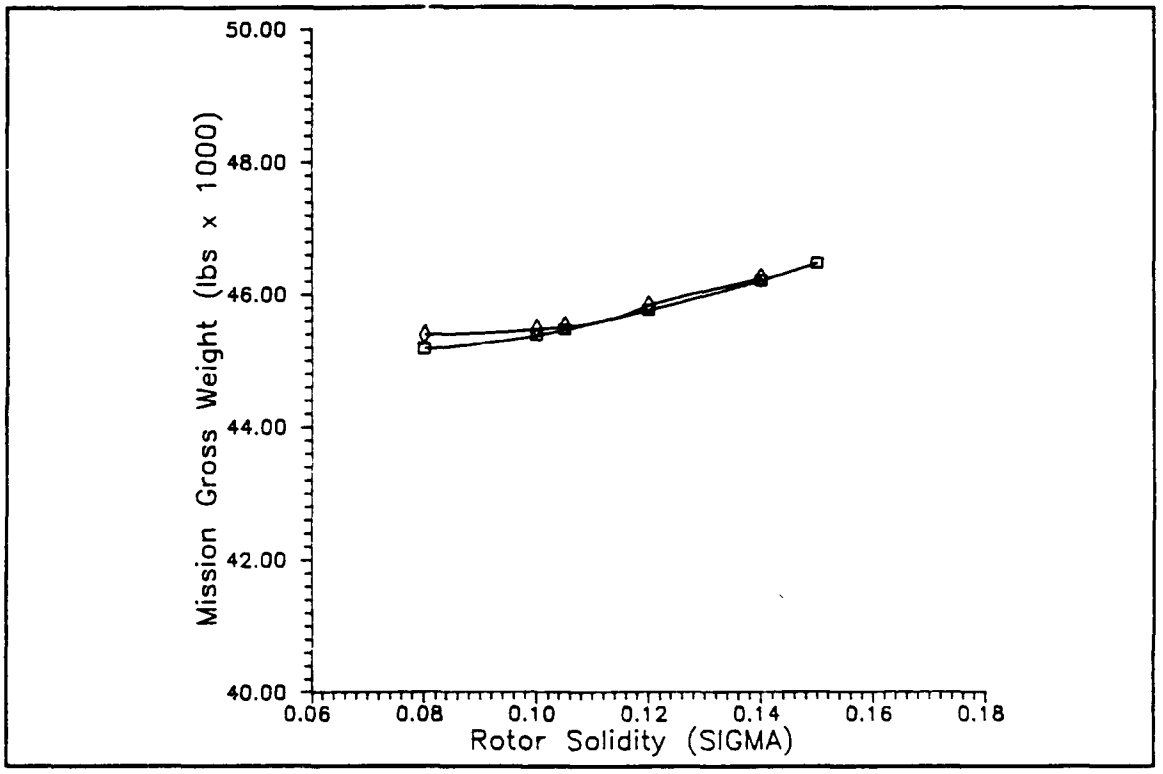

Figure 26

Mission Gross Weight
Versus Solidity

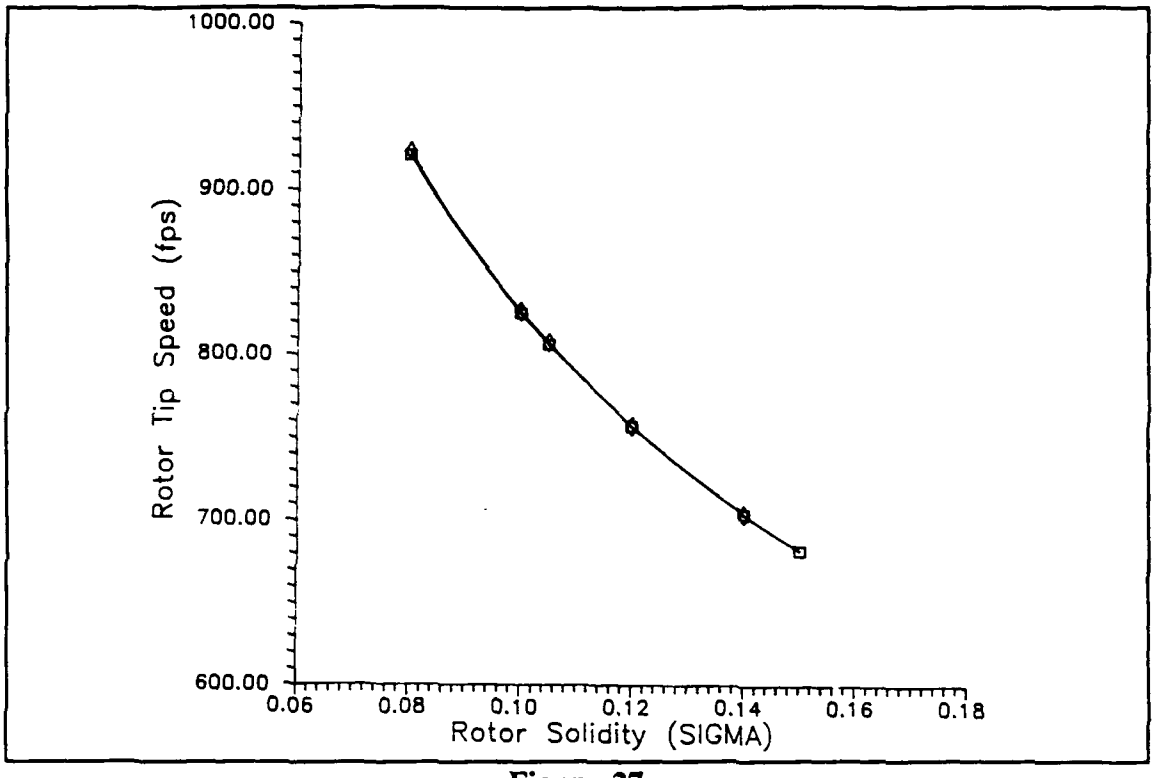

Figure 27

Tip Speed
Versus Solidity

Although there was a relative maximum in total power required (corresponding to a solidity of 0.105), the difference between the maximum and minimum values over the range studied was only 104 horsepower. As was the case for tip speed variation, the effects of solidity variation on rotor induced and profile power offset each other; but this time it was reversed. Induced power increased by 320 horsepower due to the increase in mission gross weight. As seen in Figure 28, rotor profile power decreased due to the decrease in tip speed.

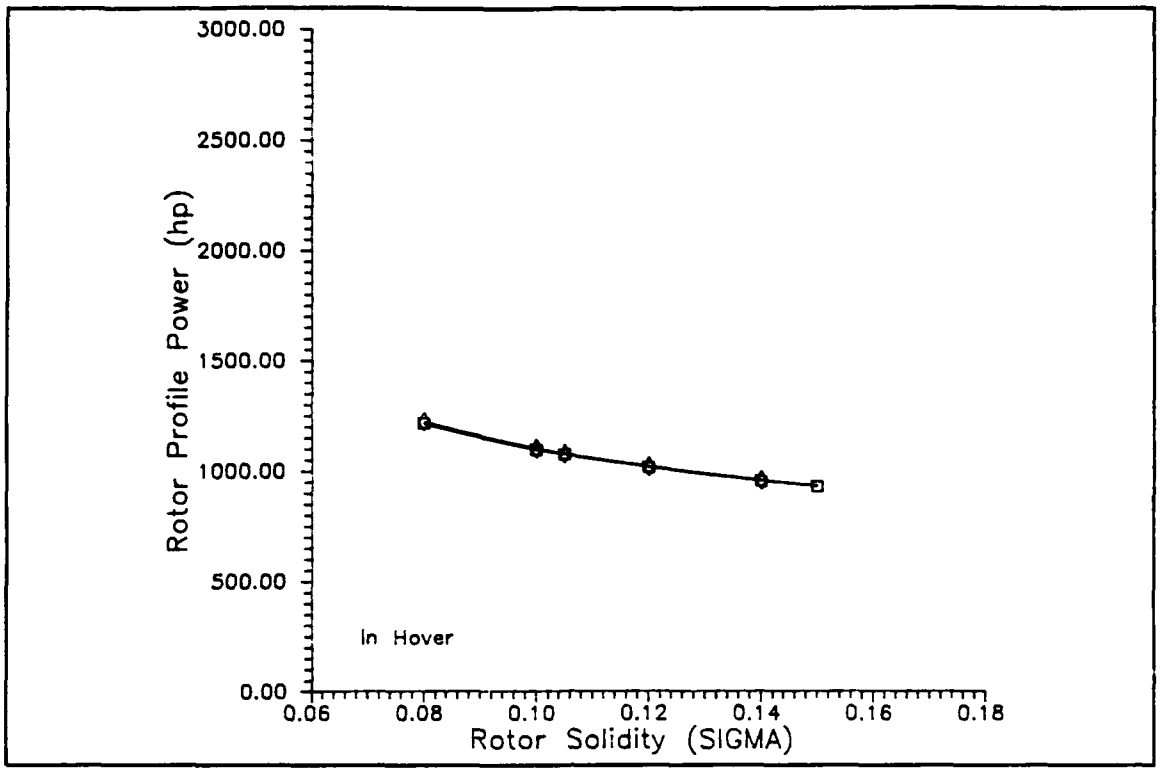

Figure 28

Profile Power
Versus Solidity

2. Aircraft Characteristics

In forward flight, the only significant effect of solidity variation was in the area of dash performance. The dash velocity decreased (by three knots) with increasing solidity. As seen in Figure 29 the increased drag associated with increased solidity led to an increase in power required. In other words, increased solidity simultaneously resulted in increased power penalty and decreased performance, however minor.

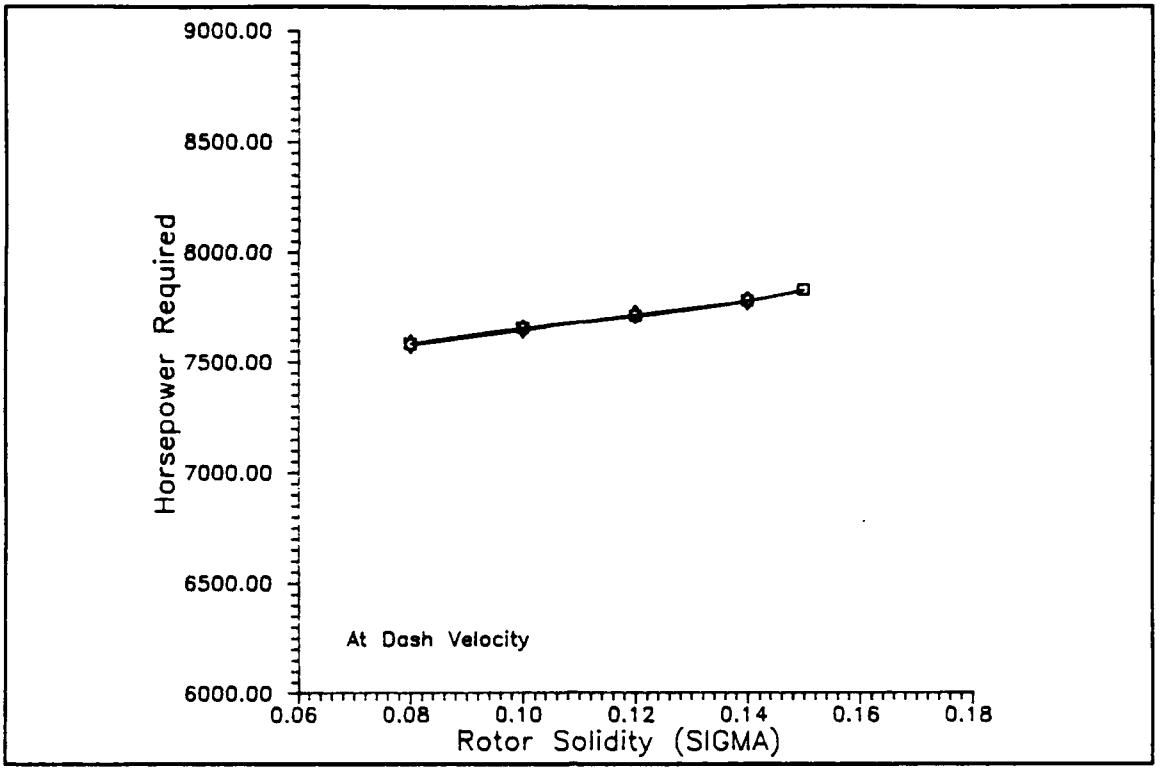

Figure 29

Dash Power Required
Versus Solidity

3. One-Engine-Inoperative (OEI) Performance

OEI climb rate for the CSAR aircraft decreased by less than 100 fpm as solidity increased; for the ASW aircraft the climb rate increased by 256 fpm. The effect of increased solidity on maximum gross weight is plotted in Figure 30. Increased solidity led to an increased weight capacity for both missions.

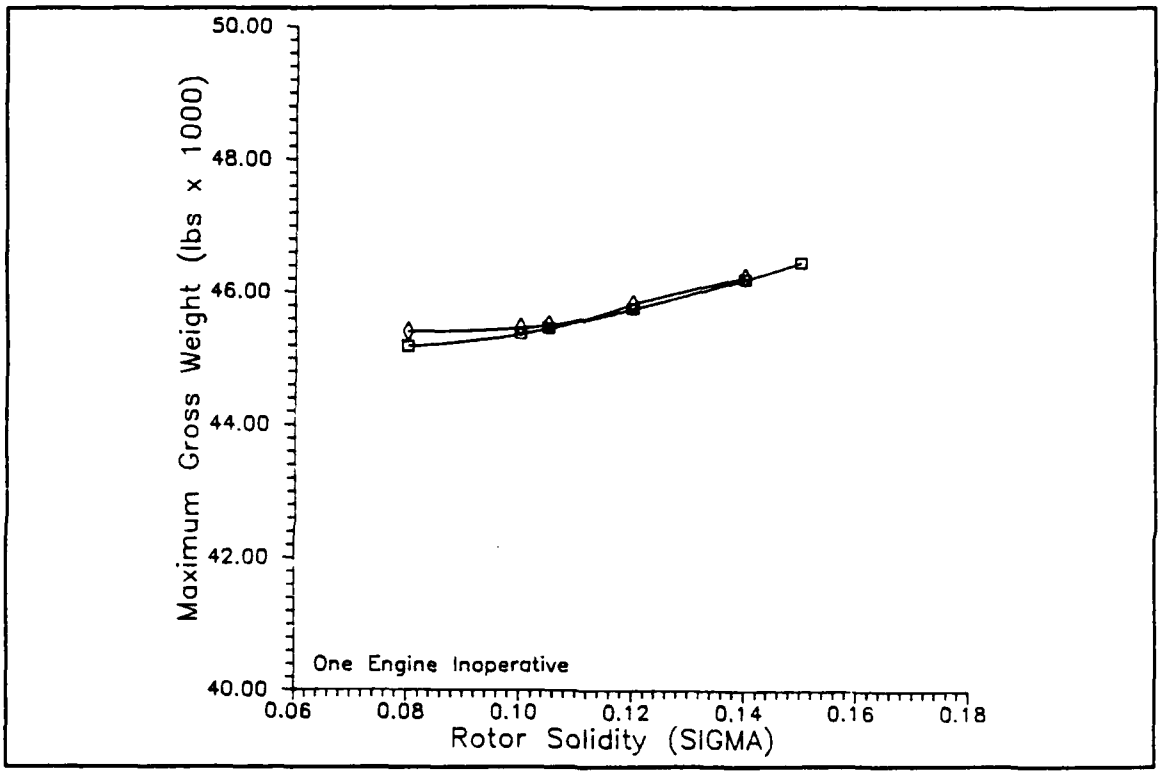

Figure 30

OEI Gross Weight
Versus Solidity

IX. VARIATION OF DOWNLOAD

Simply put, download is bad: It represents a power penalty. The question is: How much is acceptable? For instance, if a designer can achieve a desired goal by increasing disk loading or wing area, he or she needs to know at what point the gains are offset by the power penalties.

The "parameter" that was actually studied in the section was the non-dimensional ratio of (vertical drag due to) download to thrust. From this point, in order to simplify discussion, the term "download" will be used to mean the ratio of download to thrust. "Vertical drag" will be used to describe the downward force.

The value for download that was obtained in the baseline data runs was 0.111, or 11.1 percent. For analysis, downloading was varied over a range of 5 to 20 percent.

A. METHOD OF VARYING DOWNLOAD

As was previously discussed in Section IV-D, download is not a design parameter that is consciously varied. TR-87 used the Magee Download Model to calculate download based on aircraft geometry and an empirical factor (VDPRCT) that was determined experimentally for the V-22 rotor-wing combination. For the purposes of this analysis, that empirical factor was varied in the input data decks in order to get the desired range of download.

B. RESULTS OF DOWNLOAD VARIATION

Refer to Figure 8 for a legend of symbols used for the graphs in this section. Both rotor radius and blade chord were held fixed at baseline values of 19 feet and 25.04 inches. Therefore, there was no variation in aspect ratio or solidity. Disk loading changed very little over the range of download: It increased slightly from 19.89 to 20.07 psf. Tip speed was held constant at 790 fps.

As shown in Figure 31, the program predicted that mission gross weight increased with download, more so for the ASW aircraft than for the CSAR aircraft. The increase in mission gross weight was due to an increase in blade loading. Blade loading increased with the minor increase in disk loading because thrust coefficient increased while solidity was fixed. The increase was insignificant: The range of blade loading was 0.1378 to 0.1400 for the ASW mission.

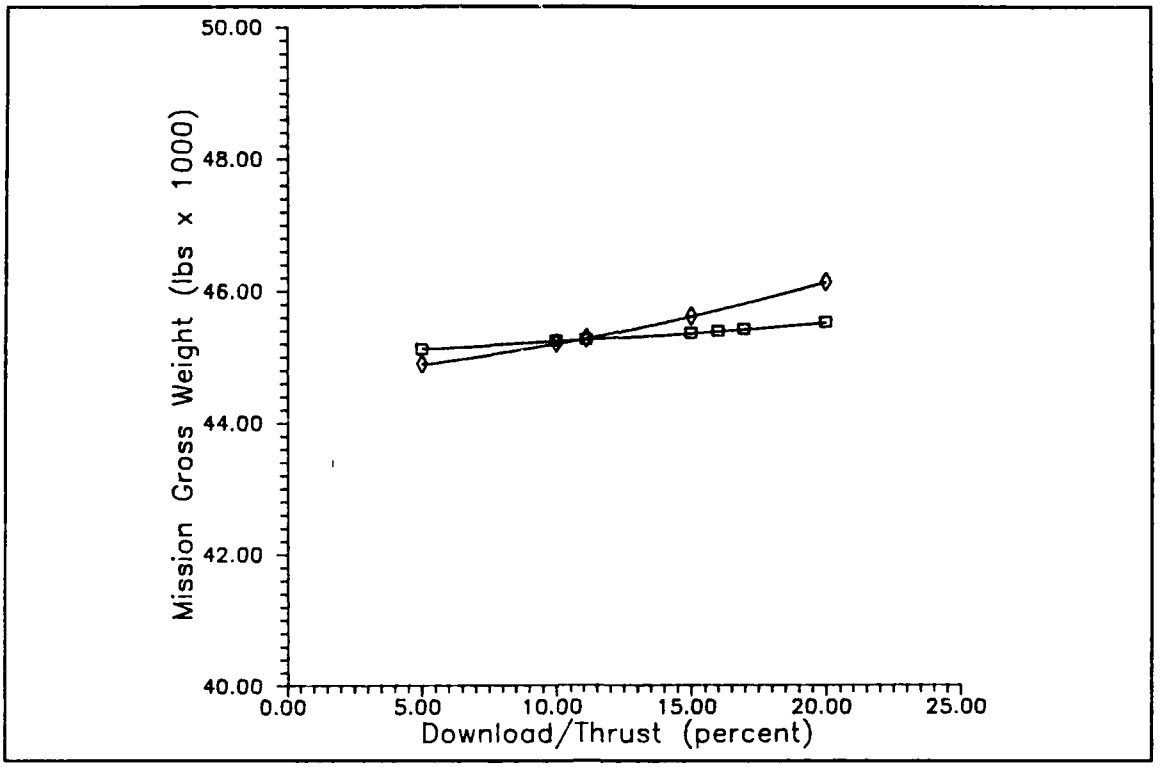

Figure 31

Mission Gross Weight
Versus Download

Figure of merit decreased with increasing download, as shown in Figure 32. One could almost have predicted a decrease intuitively; in fact, the decrease in figure of merit corresponds to an increase in both profile and induced power required for hover.

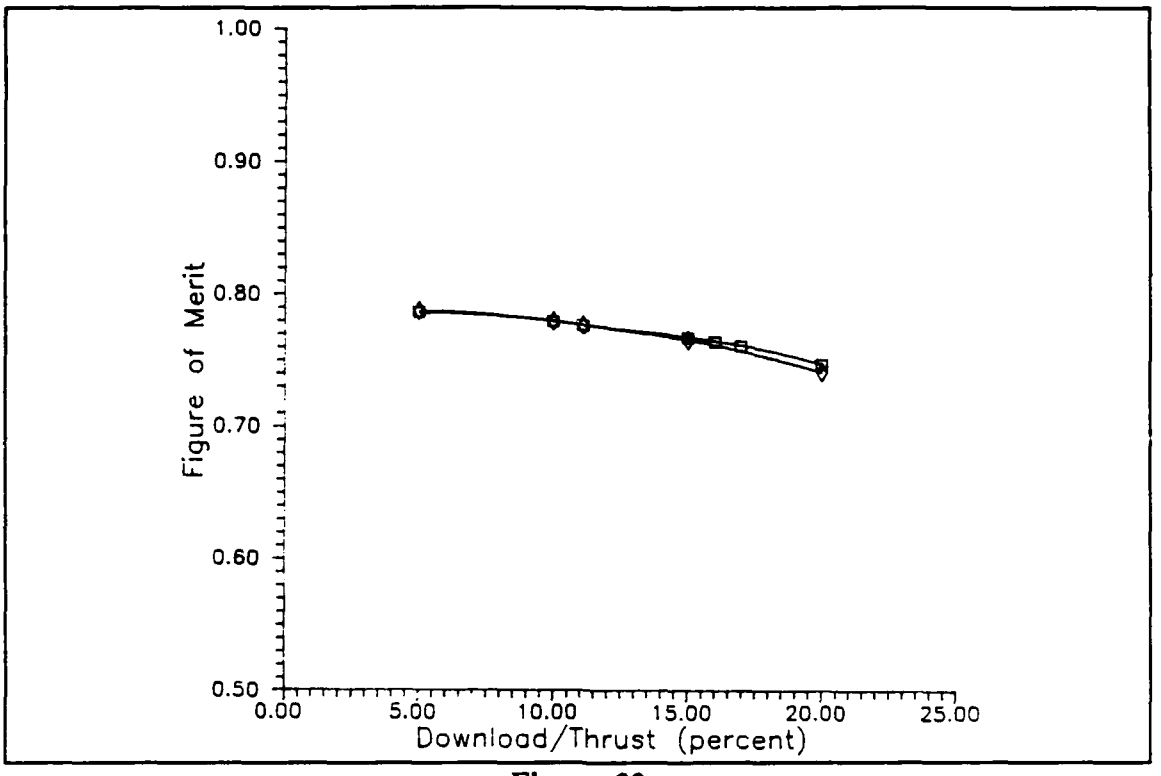

Figure 32

Figure of Merit
Versus Download

Figure 33 shows graphically the power penalties in hover due to download. (Purely) vertical climb performance would be similarly affected. In forward flight, of course, download would not be a problem. Even for a helicopter, download affects approach zero as forward flight exceeds 40 knots.

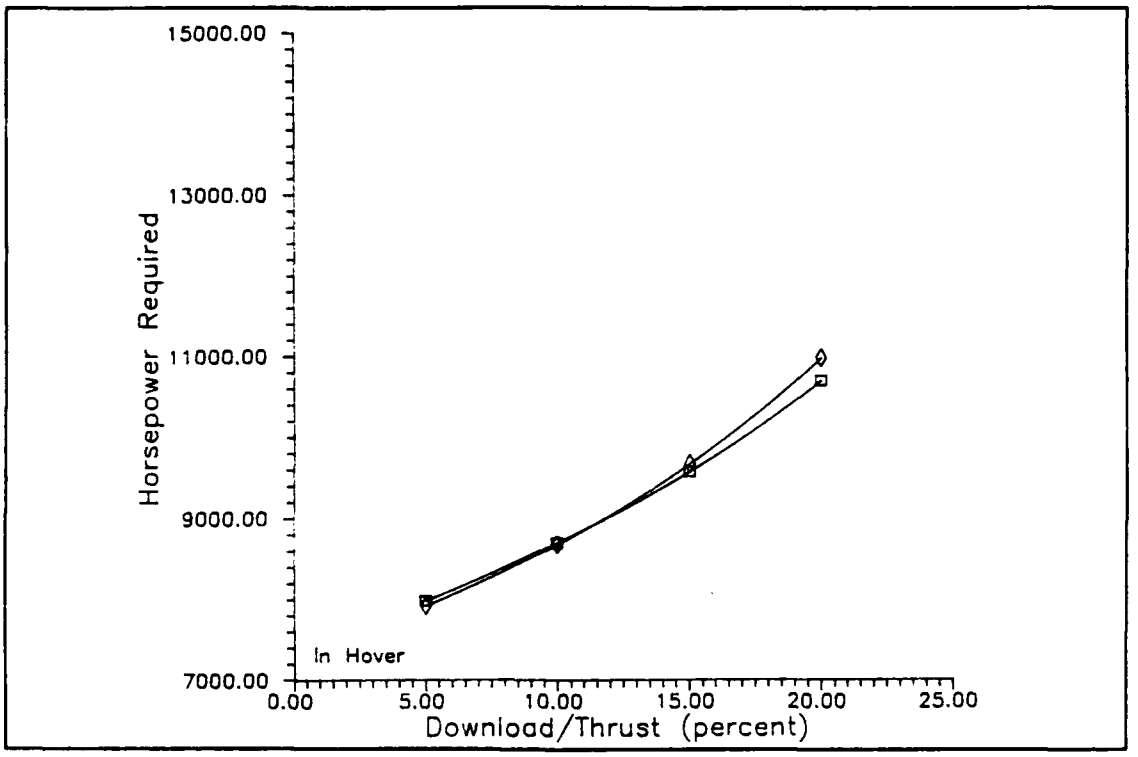

Figure 33

Hover Power Required
Versus Download

X. VARIATION OF WING LOADING

The value of wing loading for the two baseline aircraft was 118.5 psf. Wing loading was varied over a range of 70 to 180 psf.

A. METHOD OF VARYING WING LOADING

The desired values of wing loading were input to the two data decks with rotor radius, solidity, and tip speed held constant. The wing span was fixed by rotor radius; therefore, the wing chord became a fallout item.

B. RESULTS OF VARYING WING LOADING

The wing chord varied from 14.54 feet (for a wing loading of 70 psf) to 6.42 feet (for a wing loading of 160 psf). This corresponded to an increase in wing aspect ratio from 3.15 to 7.13, as compared to a baseline value of 5.5. Structural stability and flapping were not considered in this study, but would have to be considered in the design of an aircraft. Figure 8 contains a legend of symbols used to distinguish the output data.

1. Size and Rotor Characteristics

Rotor geometry was held constant. It is not immediately clear why mission gross weight varied as it did with wing loading in Figure 34. The output data shows that, as wing loading increased, wing chord decreased but wing weight increased. This is probably because the program added in weight for stiffening the wings and adding camber. On the other hand, the combined weight of the vertical

and horizontal tails decreased: This decrease in weight dominated up to a wing loading of about 100 psf.

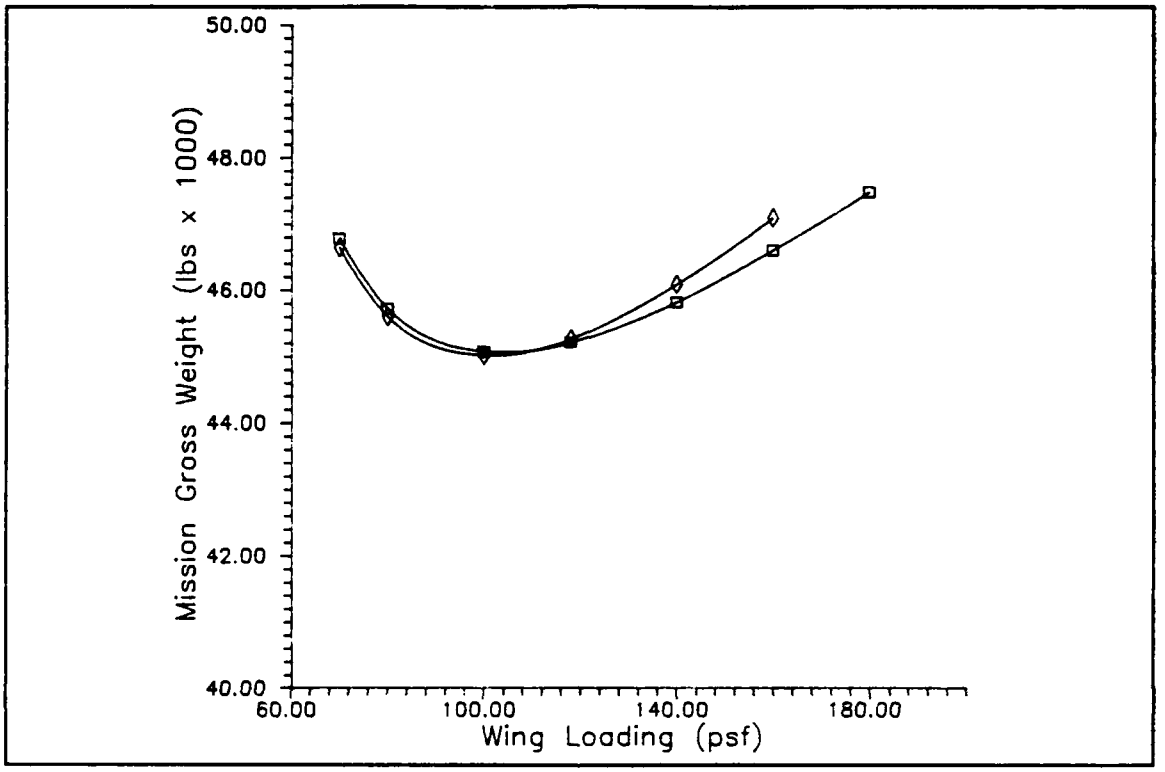

Figure 34

Mission Gross Weight
Versus Wing Loading

Another effect of increased wing loading was a substantial decrease in download. The decrease in download seen in Figure 35 can be explained by the fact that wing area decreased with increasing wing loading. Therefore, there was less flat plate drag area on which downwash impinged.

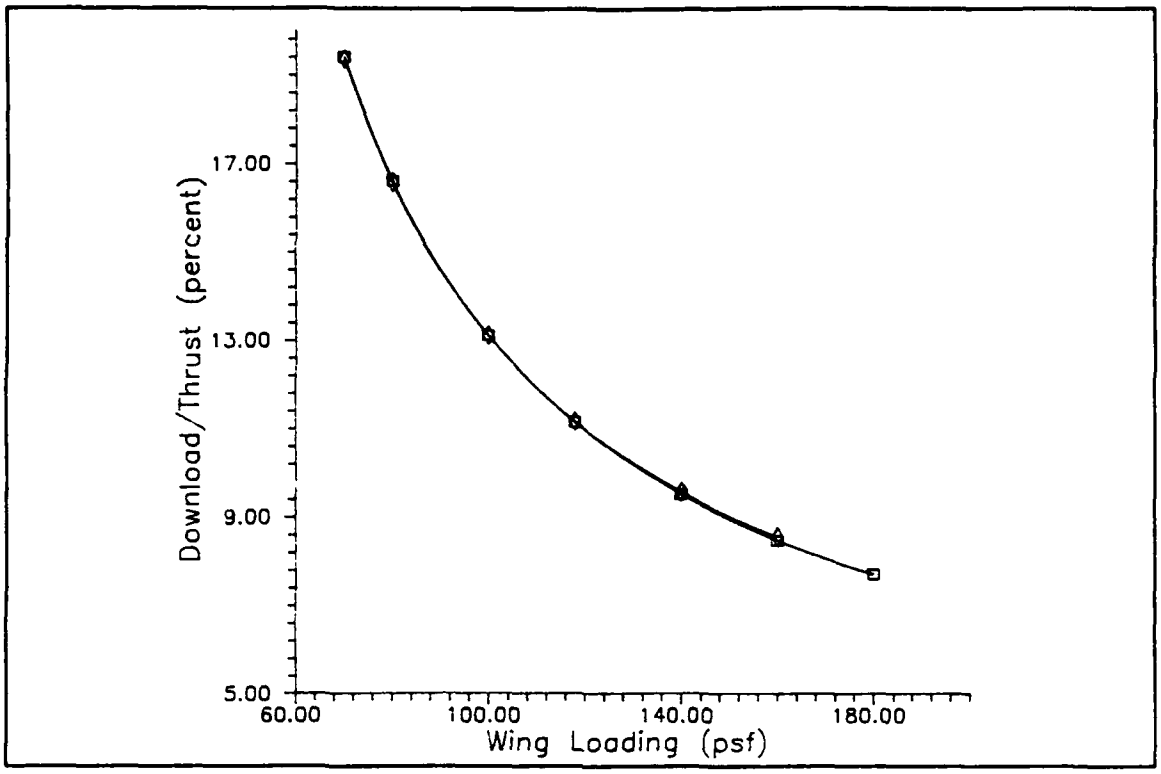

Figure 35

Download
Versus Wing Loading

The trend of rotor induced velocity in Figure 36 could be extrapolated from the trend in mission gross weight and Equation (9). In addition, rotor induced power increased by the amount necessary to overcome increased download. In Equation (13) profile power is a function of drag, density, solidity, disk area, and tip speed. Of these, the last four were fixed for the wing loading variation. Although it is not clear to the author why profile power varied as it did, Figure 37 must also be a representation of how blade drag varied with wing loading. Figure 38 shows the net effect of changes in power required for hover.

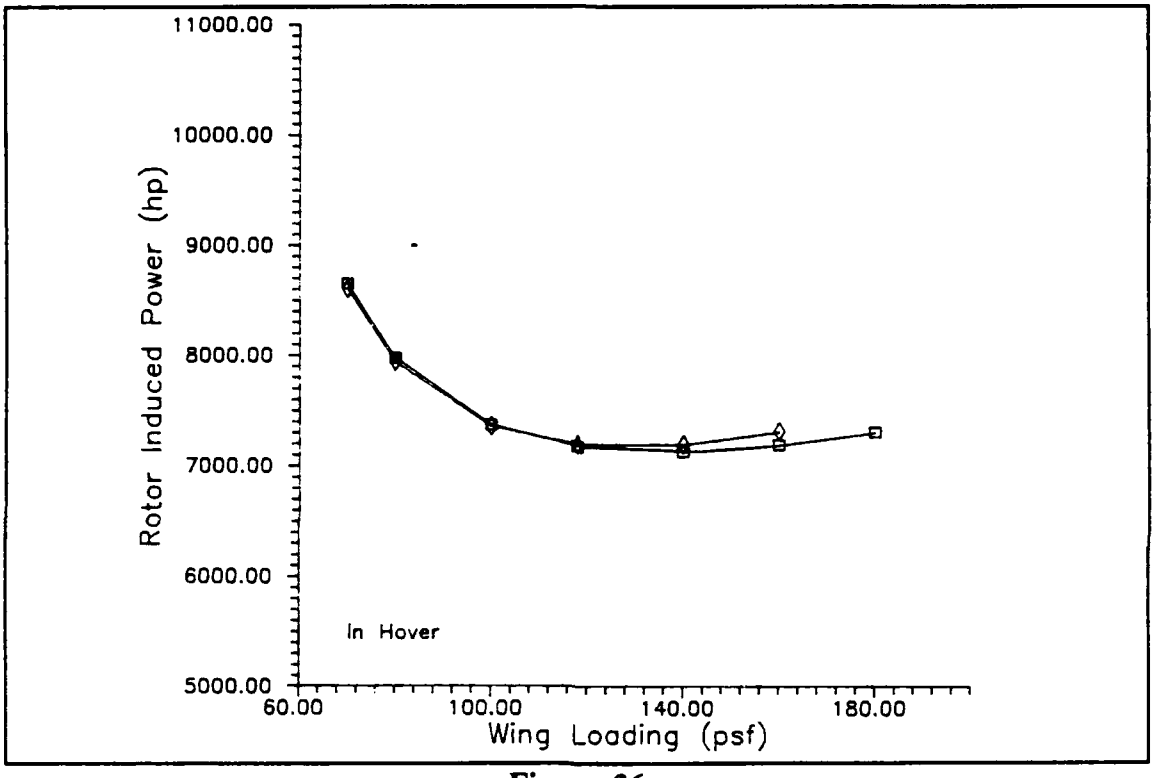

Figure 36

Rotor Induced Power
Versus Wing Loading

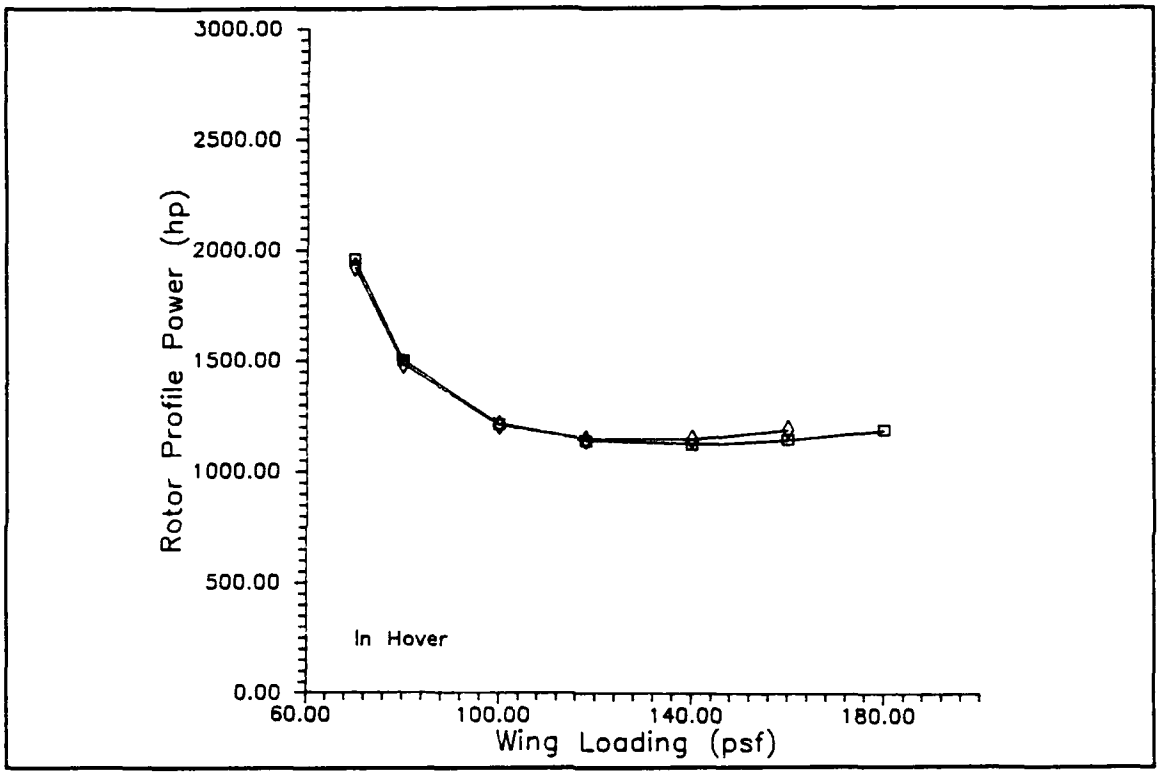

Figure 37

Profile Power
Versus Wing Loading

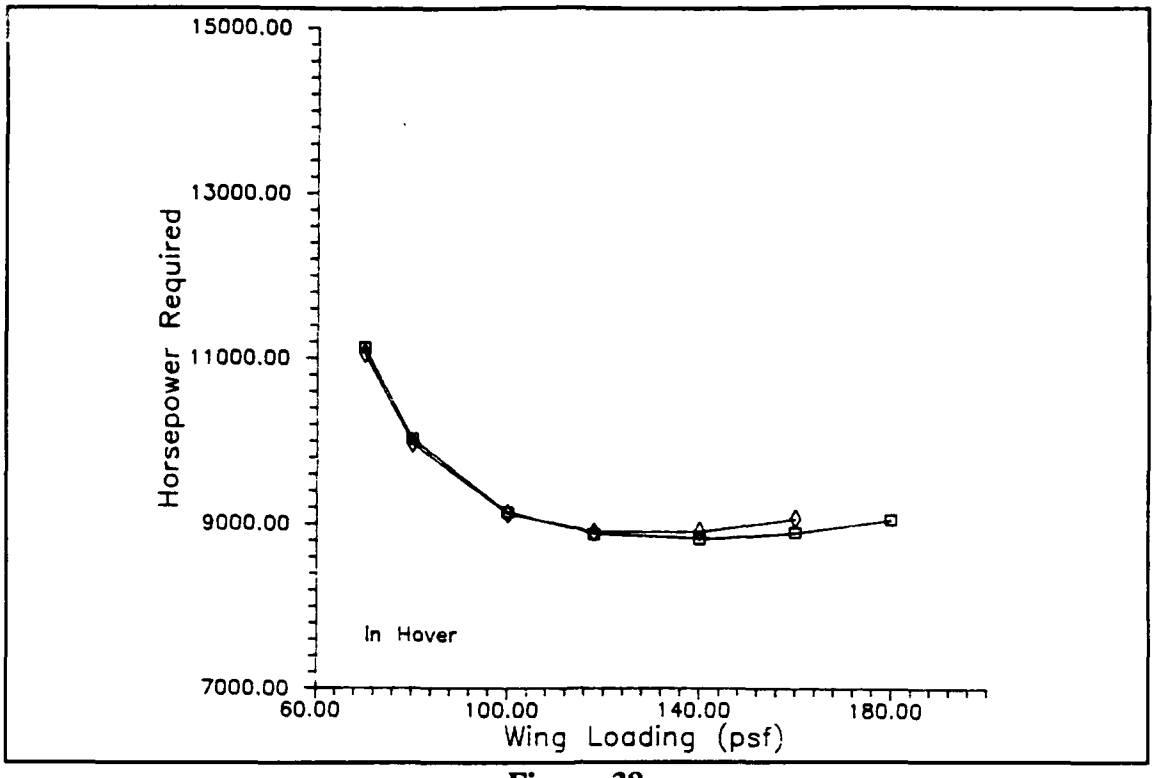

Figure 38

Total Power Required
Versus Wing Loading

2. Aircraft Characteristics

Increased wing loading resulted in increased (forward) dash performance. The data indicated no change in power required for achieving dash velocities. However, the maximum dash power increased, as shown in Figure 39. The increase was largely due to a reduction wing profile power.

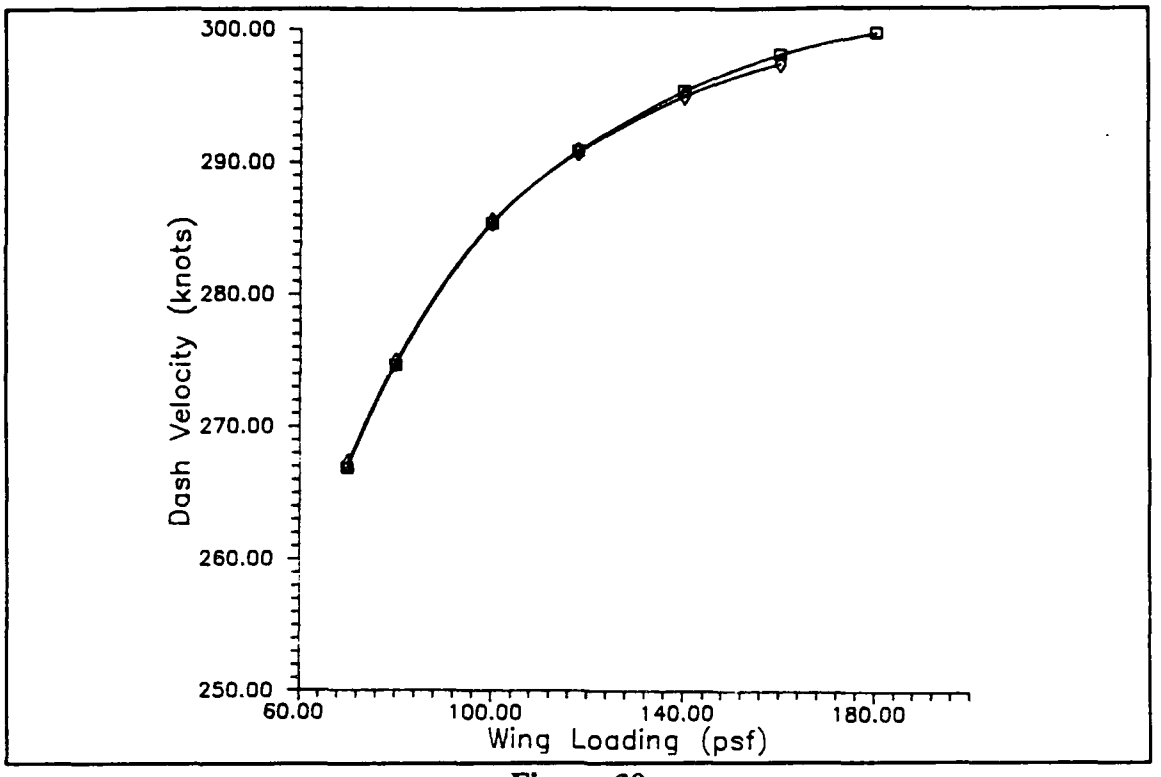

Figure 39

Dash Velocity
Versus Wing Loading

3. One-Engine-Inoperative (OEI) Performance

For the baseline disk loading, rotor size, etc., the variation of wing loading had no adverse impact on OEI weight-bearing capacity. In order to understand the behavior of OEI climb rate in Figure 40 it is necessary to review Figure 34: The climb rate is inversely proportional to the mission gross weight.

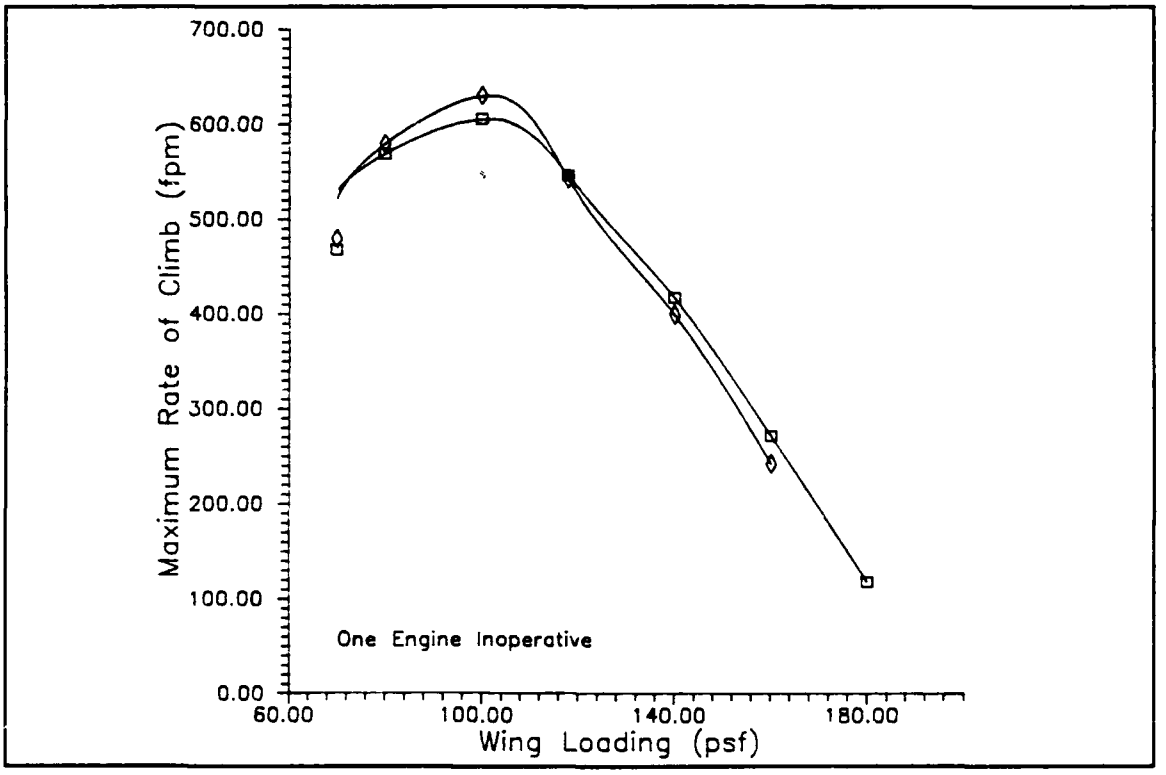

Figure 40

OEI Climb Rate
Versus Wing Loading

XI. VARIATION OF WING THICKNESS RATIO

Typical values of wing thickness ratio--the ratio of wing thickness to wing chord--are 0.06 to 0.14 for conventional airfoils. Due to structural requirements for supporting the weight of the rotors, engines, and conversion system at the outer edge of the wings, tilt-rotor wings must be thicker than for conventional aircraft. The airfoils on the V-22 Osprey have a wing thickness ratio of 0.23. The range over which wing thickness ratio was varied for this study was 0.20 to 0.26. Refer to Figure 8 for a legend of symbols used for the graphs that were generated for this analysis.

A. METHOD OF VARYING WING THICKNESS RATIO

It was possible to vary values of wing thickness ratio directly in the input data decks. Rotor radius, blade chord, and tip speed were held fixed at baseline values. Wing span was fixed because rotor radius was fixed. In addition, wing chord was fixed; therefore varying wing thickness ratio correlated directly to varying wing thickness itself. Wing thickness varied from 1.67 to 2.17 feet.

B. RESULTS OF VARYING WING THICKNESS RATIO

The most significant result of varying wing thickness ratio was the decrease in weight shown in Figure 41. As a direct result of the fixed rotor geometry and wing planform area, there were similar decreases in rotor induced power and wing loading as well, as seen in Figures 42 and 43. The reduction in gross weight was

due entirely to reduced wing weight (from 4035 to 2993 lbs): Thicker wings need fewer stiffening members and, thus, weigh less.

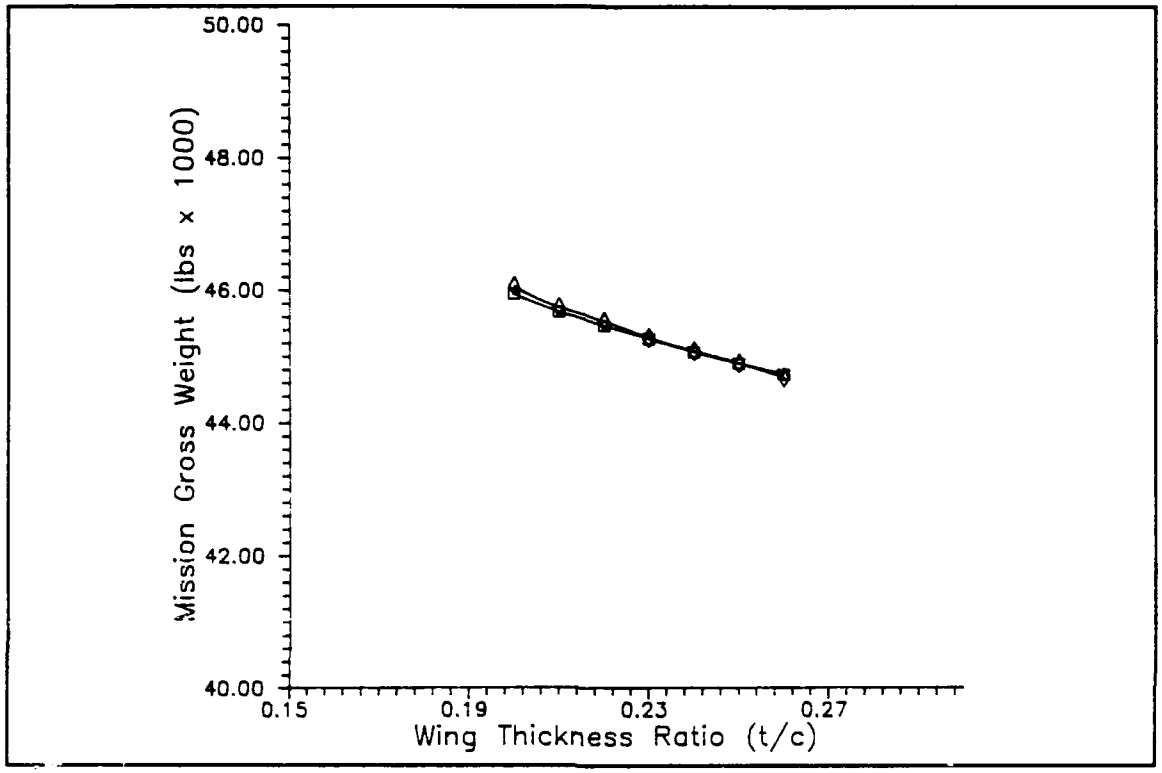

Figure 41

Mission Gross Weight
Versus Wing Thickness

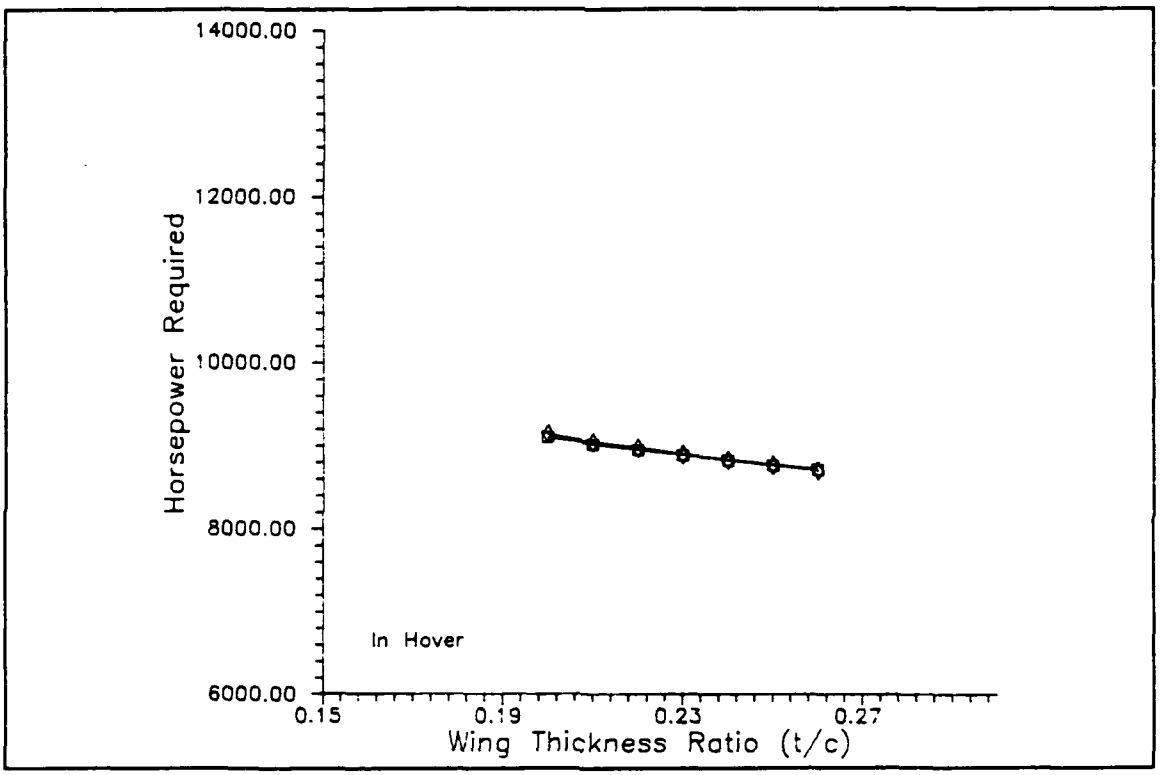

Figure 42

Hover Power Required
Versus Wing Thickness

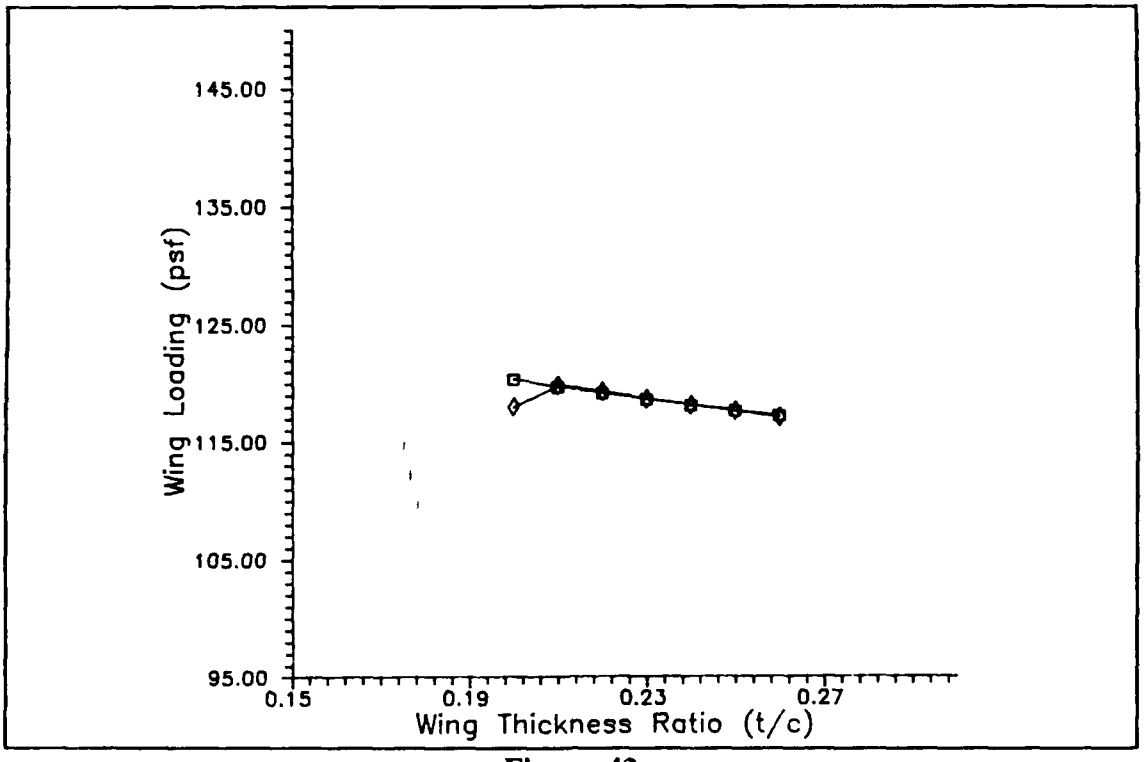

Figure 43

Wing Loading
Versus Wing Thickness

Before the analysis it was anticipated that there would be a relative minimum in mission gross weight, and that there would be an increase in power required for forward flight due to increased blunt body drag. There was an increase in power required over the range selected, but only two horsepower! The question remaining for future study is whether the analysis was not carried out for high enough wing thickness ratios or, more likely, whether the program was not able to account for the increased drag.

XII. SUMMARY AND RECOMMENDATIONS

If this study had been undertaken to seek optimum selection of parameters for a given mission, it would be appropriate at this point to draw conclusions from the results. Because this was a trend analysis, however, it will be necessary to summarize the significant results rather than make conclusions. It is hoped that the results of this project can serve as a guide to identify areas for further research in the tilt-rotor community and help to identify tilt-rotor configurations that would be suitable for a broad range of military and civil applications.

First of all, it is emphasized again that a tilt-rotor aircraft has dual modes of operation: rotary wing and conventional. Variation of two parameters--disk loading and wing loading--had the greatest impact on the elements of performance studied. This fact is not surprising. In a broad sense disk loading is the definitive parameter for rotary-wing aircraft; and wing loading is its counterpart in conventional aircraft design.

A. SUMMARY OF PARAMETER VARIATION

Disk loading variation had a significant impact on aircraft size and weight. Increased disk loading resulted in size reduction for both mission profiles. The CSAR data indicate that increased disk loading would result in lower weight over the range studied, while the ASW data reached a minimum at a disk loading of approximately 25 psf. Size reduction would draw a penalty, however: Increased

disk loading means substantial increases in hover induced velocity, download, and power required to hover.

Increasing hover tip speed resulted in a very modest decrease in mission gross weight and a similarly modest increase in power required to hover Compressibility effects and retreating blade stall are not as restrictive for a tilt rotor as for a helicopter because the tilt rotor converts to "conventional" forward flight. Therefore, selection of tip speed for a tilt rotor would largely be a tradeoff between weight and power, with noise and vibration taken into account.

Increasing solidity resulted in a fairly significant reduction in tip speed, which would be beneficial if noise reduction were desired. On the other hand, a modest weight increase occurred. If increased maneuverability and low noise signature were design requirements, some weight penalty might be acceptable.

It has already been stated that selection of download is not actually part of the design process. The adverse effects of download would have to be considered when selecting values for other parameters.

The influence of wing loading variation was almost the reverse of the disk loading case. Increased wing loading resulted in a minimum weight; there was a steady increase in mission gross weight for wing loading values above 100 psf. However, increased wing loading resulted in a substantial reduction in download; further, there was a reduction in power required to hover up to 140 psf, with only a shallow rate of increase beyond that value.

Finally, the increased wing thickness ratio resulted in a modest decline in gross weight with virtually no power penalty. The discussion in Section XI ended with a

question concerning the ability of the computer program to accurately gauge the effects of increasing the wing thickness. That question is a lead-in for recommendations for further study.

B. RECOMMENDATIONS FOR FUTURE WORK

This study is actually an interim report: It is intended to be a temporary measure to help fill the gap between the limited amount of current information available on the XV-15 and V-22 and future flight test information the V-22 and different tilt-rotor variants. Also, this study obviously just begins to "scratch the surface" of work that could be done. Recommendations for future work include:

- more in-depth dynamic performance analyses;
- optimization studies for specific mission profiles;
- integrate wake vortex models into the rotor performance subroutine of TR-87; and,
- comparison of results with V-22 flight data (when available) and further correlation of TR-87.

LIST OF REFERENCES

1. *Technology Assessment of Capability for Advanced Joint Vertical Lift Aircraft (JVX) Summary Report,* Analysis and preparation chaired by Aviation Research and Development Command (AVRADCOM), May 1983.

2. Johnson, W., Lau, B. H., and Bowles, J. V., *Calculated Performance, Stability, and Maneuverability of High-Speed Tilting-Prop-Rotor Aircraft,* paper presented at the European Rotorcraft Forum, 12th, Garmisch-Partenkirchen, 22-25 September 1986.

3. Johnson, Wayne, *Helicopter Theory,* Princeton University Press, 1980.

4. Felker, F. F., Maisel, M. D., and Betzina, M. D., *Full-Scale Tilt-Rotor Hover Performance,* paper presented at the Annual Forum of the American Helicopter Society, 41st, Fort Worth, Texas, May 1985.

5. Stepniewski, W. Z., and Keys, C. N., *Rotary-Wing Aerodynamics,* Dover Publications, Inc., 1984.

6. Prouty, R. W., *Helicopter Aerodynamics,* PJS Publications, Inc., 1985.

7. Layton, D. M., *Helicopter Performance,* Matrix Publishers, Inc., 1984.

8. *Engineering Design Handbook,* Headquarters, Army Material Publications Command, AMCP 706-201.

9. Roskam, J., *Airplane Design,* Roskam Aviation and Engineering Corporation, Ottawa, Kansas, 1985.

INITIAL DISTRIBUTION LIST

1.	Defense Technical Information Center Cameron Station Alexandria, VA 22304-6145	2
2.	Library, Code 0142 Naval Postgraduate School Monterey, CA 93943-5002	2
3.	Mr. Fort F. Felker Rotary-Wing Aeromechanics Branch Mail Stop T-31 NASA-Ames Research Center Moffett Field, CA 94035	5
4.	CDR Hugh Sheehy Rotary-Wing Aeromechanics Branch Mail Stop T-31 NASA-Ames Research Center Moffett Field, CA 94035	1
5.	CDR Roger Vehorn Naval Air Systems Command PMA-275 Washington, DC 20361-1275	1
6.	CDR Steve Fahrenkrog Naval Air Systems Command PMA-275 Washington, DC 20361-1275	1
7.	Dr. E. Robert Wood, Chairman Department of Aeronautics and Astronautics Code 67 Naval Postgraduate School Monterey, CA 93943	1
8.	Prof. R. D. Wood Department of Aeronautics and Astronautics Code 67WR Naval Postgraduate School Monterey, CA 93943	2

9. Prof. R. M. Howard — 1
Department of Aeronautics and Astronautics
code 67HO
Naval Postgraduate School
Monterey, CA 93943

10. Prof. R. Kolar — 1
Department of Aeronautics and Astonautics
Code 67KJ
Naval Postgraduate School
Monterey, CA 93943

11. Dr. Mike Scully — 1
Headquarters, USA Aviation Research and Technology Activity
Code XA
Mail Stop 219-3
NASA-Ames Research Center
Moffett Field, CA 94035-1099

12. Mr. John Davis — 1
Headquarters, USA Aviation Research and Technology Activity
Code XA
Mail Stop 219-3
NASA-Ames Research Center
Moffett Field, CA 94035-1099

13. Bell Boeing V-22 Joint Project Office — 2
Suite 401 Crystal Gateway One
1235 Jefferson Davis Highway
Arlington, VA 22202

14. LT Mary C. Dunston — 2
Air Test and Evaluation and Squadron ONE
Naval Air Station
Patuxent River, MD 20670-5305